Flow-mediated effects on travel time, routing, and survival of juvenile Chinook salmon in a spatially complex, tidally forced river delta

Russell W. Perry[1*], Adam C. Pope[1], Jason G. Romine[1**], Patricia L. Brandes[2], Jon R. Burau[3], Aaron R. Blake[3], Arnold J. Ammann[4], and Cyril J. Michel[4]

[1] U.S. Geological Survey, Western Fisheries Research Center, 5501A Cook-Underwood Road, Cook, WA 98605, USA (RWP: rperry@usgs.gov; ACP: apope@usgs.gov; JRG: jason_romine@fws.gov)

[2]U.S. Fish and Wildlife Service, 850 Guild Ave, Suite 105, Lodi, CA 95240, USA (PLB: pat_brandes@fws.gov)

[3]U.S. Geological Survey, California Water Science Center, 6000 J Street, Placer Hall, Sacramento, CA 95819, USA (JRB: jrburau@usgs.gov; ARB: ablake@usgs.gov)

[4]National Marine Fisheries Service, Southwest Fisheries Science Center, 110 Shaffer Rd., Santa Cruz, CA 95060, USA (AJA: arnold.ammann@noaa.gov; CJM: cyril.michel@noaa.gov)

[*]Corresponding author:

Phone: 509-538-2942

Fax: 509-538-2843

** Present address: U.S. Fish & Wildlife Service, Mid-Columbia River National Wildlife Refuge Complex, 64 Maple St, Burbank, WA 99323, USA

Abstract

We evaluated the interacting influences of river flows and tides on travel time, routing, and survival of juvenile late-fall Chinook salmon (*Oncorhynchus tshawytscha*) migrating through the Sacramento-San Joaquin River Delta. To quantify these effects, we jointly modeled the travel time, survival, and migration routing in relation to individual time-varying covariates of acoustic-tagged salmon within a Bayesian framework. We used observed arrival times for detected individuals and imputed arrival times for undetected individuals to assign covariate values in each reach. We found travel time was inversely related to river inflow in all reaches, yet survival was positively related to inflow only in reaches that transitioned from bidirectional tidal flows to unidirectional flow with increasing inflows. We also found that the probability of fish entering the interior Delta, a low-survival reach, declined as inflow increased. Our study illustrates how river inflows interact with tides to influence fish survival during the critical transition between freshwater and ocean environments. Furthermore, our analytical framework introduces new techniques to formally integrate over missing covariate values to quantify effects of time-varying covariates.

Introduction

Anadromous salmonids have evolved diverse life history strategies that capitalize on spatial and temporal variation in their habitat to maximize productivity. Understanding how salmonids use habitat over space and time can provide insight into population dynamics and help to identify particularly sensitive stages in their life history. Regulated rivers influence migrations of anadromous salmonids by altering the timing, magnitude, variation, and constituents of river discharge (e.g., temperature, turbidity), which in turn can affect their survival (Raymond 1988; Smith et al. 2003). Thus, interest often centers on how regulation of river flow affects survival of juvenile salmonids at different locations and times (Skalski et al. 2002; Michel et al. 2015).

Juvenile Chinook salmon (*Oncorhynchus tshawytscha*) in the Central Valley of California, USA, emigrate from natal tributaries of the Sacramento River through the Sacramento-San Joaquin River Delta (henceforth, "the Delta"), a network of natural and man-made channels linking the Sacramento and San Joaquin rivers to San Francisco Bay and the Pacific Ocean (Fig. 1). The Delta is the hub of California's water delivery system, providing agricultural and domestic water that supports California's economy, the eighth largest in the world (Healey et al. 2016). Water from the Sacramento River is diverted from the North through natural channels and gated man-made channels to the South where large pumping stations "export" water from the Delta in canals (Fig. 1). As juvenile salmon enter the Delta, they distribute among its complex channel network where they are subject to channel-specific abiotic and biotic factors that influence their migration timing, growth, and survival. For example, fish that enter the interior Delta, the region to the south of the mainstem Sacramento River (reach 8 in Fig. 1), survive at lower rates than fish migrating through northerly routes, likely owing to longer

travel times, longer travel distances, higher predation rates, and entrainment at the pumping stations (Brandes and McLain 2001; Newman and Brandes 2010; Perry et al. 2010, 2013).

Survival of juvenile salmon has been positively related to river discharge at the Delta-wide scale (Kjelson et al. 1982; Kjelson and Brandes 1989; Newman and Rice 2002; Newman 2003), but the underlying factors driving this relationship remain unclear. Low river discharge has been associated with a high proportion of fish entering the interior Delta, thereby decreasing overall survival by subjecting a larger fraction of the population to low survival probabilities (Perry et al. 2015). What remains unclear is the extent to which within-reach survival contributes to the overall flow-survival relationship. Is survival related to discharge in all reaches, or do a few key reaches drive the overall flow-survival relationship? Given that the Delta transitions from unidirectional flow in its upper reaches to tidally driven bidirectional flows in lower reaches, we hypothesized that the reach-specific relationship between inflow and survival could vary along this gradient. Understanding exactly which reaches contribute to the overall flow-survival relation will help researchers to focus on specific mechanisms driving this relationship and help managers to target specific actions to increase survival.

Here, we analyze acoustic telemetry data on juvenile Chinook salmon from 17 distinct release groups collected from two studies conducted between 2007 and 2011 (Table 1) to understand how reach-specific travel time, migration routing, and survival vary among reaches in the Sacramento-San Joaquin River Delta. Because each release group spread out over time as they migrated through the Delta, individuals entered a given reach over a wide range of environmental conditions. Our interest therefore centered on quantifying factors affecting individual variation in survival. However, time-varying individual covariates are a vexing problem in conventional mark-recapture models (e.g., maximum likelihood estimation performed

in Program Mark, White and Burnham 1999) because the value of the covariate is unknown when an individual is undetected, rendering the likelihood analytically intractable in most cases (but see Catchpole et al. 2008). Therefore, we developed a Bayesian hierarchical model that jointly modeled both travel times and survival of juvenile salmon. The travel time model was used to impute arrival times of undetected fish in each reach, which allowed us to define covariate values based on imputed arrival times for undetected individuals. We then used Markov Chain Monte Carlo techniques to integrate the likelihood over the missing covariate values while simultaneously estimating parameters associated with both travel time and survival.

Methods

Study area and telemetry system

The telemetry system was designed to accommodate requirements of a multistate mark-recapture model that estimated reach- and route-specific survival for nine discrete reaches and four primary migration routes through the Delta (Perry et al. 2010; Figs. 1 and 2). The nine reaches separate the Delta into the three hydrodynamic zones: 1) riverine reaches with unidirectional flows and the least influence of tidal forcing (reaches 0–2), 2) transitional reaches that shift from unidirectional flow to tidally driven bidirectional flows as river flow entering the Delta decreases (reaches 3–6), and 3) tidal reaches with bidirectional flows regardless of the amount of river flow entering the Delta (reaches 7–8, Figs. 1 and 3). These nine reaches comprise four distinct migration routes that constitute the states of the multistate model: the Sacramento River (Route A = reaches 1, 2, 4, and 7), Sutter and Steamboat Slough (Route B = reaches 1, 3, and 7), the Delta Cross Channel (Route C = reaches 1, 2, 6, and 8), and Georgiana Slough (Route D = reaches 1, 2, 5, and 8; Figs. 1 and 2).

Each telemetry station consisted of single or multiple tag-detecting monitors (Vemco Model VR2, Amirix Systems, Inc., Halifax, Nova Scotia, Canada), depending on the number of monitors needed to maximize detection probabilities at each station. Migration routes A, B, C, and D were monitored with 7, 1, 1, and 2 telemetry stations, respectively, labeled according to migration route *r* at sampling occasion *j* (Figs. 1 and 2). Sampling occasion was defined based on the *j*th telemetry station within the mainstem Sacramento River, with the upstream release site defined as occasion one. Migrating juvenile salmon first arrive at Sutter and Steamboat Slough (B_3), which diverges from the Sacramento River at the first river junction and converges again with the Sacramento River upstream of A_5 (Figs. 1 and 2). Fish remaining in the Sacramento River then pass the Delta Cross Channel (C_4), a man-made gated canal that diverts fish, when its gates are open, into reach 6 and subsequently into the interior Delta (reach 8). The Delta Cross Channel is used to control salinity at the water pumping stations, undergoes mandatory closures for fisheries protection in mid-December each year, and also closes when Sacramento River flow exceeds 708 $m^3 \cdot s^{-1}$ (25,000 $ft^3 \cdot s^{-1}$). Fish then pass Georgiana Slough (D_4), a natural channel (reach 5) that also leads to the interior Delta (reach 8). All routes then converge at Chipps Island (A_6), the terminus of the Delta. With this configuration, survival to site A_6 is confounded with detection probability at the last telemetry station. Therefore, to estimate survival to A_6, we pooled detections from numerous tag detecting monitors downstream of A_6 in San Francisco Bay for estimating detection probability at Chipps Island.

Although there are numerous possible migration pathways, we focused on these four routes because management actions likely have the largest influence on movement and survival among these routes. For example, fish may enter the interior Delta from the Sacramento River through either Georgiana Slough or the Delta Cross Channel, where they subsequently become

vulnerable to migration delays and entrainment at the water pumping projects (Perry et al. 2010; Newman and Brandes 2010). Steamboat and Sutter Slough is an important migration route because fish using this route bypass the Delta Cross Channel and Georgiana Slough (Fig. 1) thereby avoiding the interior Delta. Thus, monitoring these primary migration routes provides information about the likely ultimate fate of individuals.

Fish tagging and release

All juvenile late fall Chinook salmon were obtained from the Coleman National Fish Hatchery in Anderson, California. Release groups were defined based on release timing and data source, with the exception of release group 3, which was pooled over a longer period of release times owing to small sample size (Table 1). All fish other than release group 1 were tagged with a 69 kHz acoustic tag weighing 1.58 g (Vemco Model V7-2L-R64K, Amirix Systems, Inc., Halifax, Nova Scotia, Canada) transmitting either every 30–90 s (release groups 1–3) or 15–60 s (release groups 4–17). Battery life of these transmitters ranged from 98–749 d based on tests conducted by Michel et al. (2015). Fish from release group 1 were tagged with an acoustic tag weighing 1.44 g, which had an expected battery life of 70 d (Vemco Model V7-2L-R64K).

Most juvenile salmon were surgically tagged at the hatchery and then transported to release sites, but fish from release groups 8 and 11 were tagged at release sites. Fish were randomly selected and those ≥140 mm fork length were retained for tagging to maintain tag burden below 6% of the fish weight. Fish tagged by Michel et al. (2015) were held at the hatchery for 24 h following surgery, transported to release sites, and held in-river for 1–3 h prior to release. Fish tagged by Perry et al. (2010, 2012, 2013) fish were transported to release sites, held in-river at release sites for 24 h, and then released into either the Sacramento River near

Sacramento, CA (n_{A1}) or Georgiana Slough (n_{D4} ; Fig. 1 and 2). Fish were released into Georgiana Slough to increase the number of fish entering the interior Delta (reach 8) and improve precision of survival estimates for that region. For the Michel et al. (2015) study, fish were released well upstream of the Delta, at four locations in the Sacramento River (Table 1). In most migration years, two releases were made; one in December and another in January. Releases in December occurred prior to seasonal closure of the Delta Cross Channel gates, which typically occurs on December 15; whereas the Delta Cross Channel gates were closed for all January releases. Further details of tagging and release protocols can be found in the citations listed in Table 1.

Screening for false positive detections and predators

Telemetry data were screened for false positive detections by first summarizing data into detection events defined by the number of consecutive detections from an individual tag within a 30-minute period at a given telemetry station. Any detection event with at least two detections at a given location was considered as valid. Detection events with a single detection were considered valid if the detection was consistent with the entire spatiotemporal detection history of the individual's tag (e.g., a single detection was preceded by an upstream detection and proceeded by a downstream detection). Otherwise, single detections were considered false positives and removed from analysis.

Tags that may have been consumed by predators were identified by adapting the methods of Gibson et al. (2015), which consisted of several steps. First we calculated five movement metrics from tag detections that quantified differences in behavioral patterns between live tagged smolts and tagged smolts that had been consumed by predators such as striped bass (*Morone*

saxatilis), smallmouth bass (*Micropterus dolomieu*), largemouth bass (*Micropterus salmoides*), and spotted bass (*Micropterus punctulatus*). The metrics included: 1) the mean rate of downstream movement calculated as the shortest channel distance between consecutive detections of downstream movements divided by the elapsed time between detections, 2) the number of consecutive detection events occurring at the same location, 3) the cumulative distance travelled divided by the total number of days spent in the study area, 4) the number of transitions between telemetry stations that were deemed to be only possible by a predator (i.e., movement upstream against the flow), and the total time in the array from the time of release to the time of last detection.

Next we used hierarchical cluster analysis to group each tag by the multivariate characteristics of the five metrics. We used the hclust package in R (R Core Team 2015) and divided the tags in three groups based on the dendrogram resulting from hierarchical clustering using Ward's minimum variance method (Ward 1963; Gibson et al. 2015). We then selected the group whose movement characteristics were most consistent with that of predator-like behavior (i.e., upstream movement against flow, long residence times near receivers, and low average distance travelled per day). We examined each tag's time series of movement metrics to identify if and when the tag transitioned from smolt-like to predator-like behavior. The detection history was then truncated at this point in the detection history. Overall, 17% percent of tags were flagged for review based on the movement metrics, and 11% percent exhibited predator-like behavior that required truncation of their capture history.

Structure of the mark-recapture model

175 The multistate mark-recapture model estimates three types of parameters from detections
176 of acoustic-tagged juvenile Chinook Salmon: $S_{r,j}$ is the probability of surviving from a
177 telemetry station within route *r* at sampling occasion *j* to the next downstream telemetry station;
178 $\Psi_{r,s,j}$ is the probability of entering route *s* from route *r* at sampling occasion *j*, conditional on
179 surviving to occasion *j* (henceforth, routing probability); and $P_{r,j}$ is the probability of detecting a
180 tagged fish at a telemetry station on sampling occasion *j* within route *r*, conditional on fish
181 surviving to occasion *j* (Fig. 2). In the parlance of multistate mark-recapture models, the routes
182 constitute the states, the routing probabilities represent the state transition probabilities, and
183 survival and detection probabilities are conditioned on migration route (i.e., conditioned on
184 state).

185 In addition, our modeling framework includes an auxiliary model for travel times, which
186 we used to impute arrival times of undetected individuals in each reach for the purposes of
187 assigning daily covariate values. This model estimates two travel time parameters associated
188 with lognormally distributed travel times: $\mu_{r,j}$ is the mean of log-travel times from a telemetry
189 station in route *r* at sampling occasion *j* to the next downstream telemetry station, and $\sigma^2_{r,j}$ is the
190 variance of the travel times. Because reaches 1–8 are associated with a unique *r*, *j* combination
191 (route, sampling occasion) we generally refer to travel time and survival parameters as being
192 reach-specific (Fig. 1 and 2).

193 To understand how both migration routing and reach-specific survival contribute to
194 overall survival through the Delta, we model the underlying parameters as functions of
195 covariates and then reconstruct the overall relationship from these component parts. Overall
196 survival through the Delta was reconstructed from the individual components as:

197 (1) $$S_{\text{Delta}} = \sum_{r \in \{\text{A,B,C,D}\}} \Psi_r S_r$$

198 where S_r is the survival from telemetry stations A_2 to A_6 (i.e., from the entrance to the exit of
199 the Delta) for fish taking migration route *r*, and Ψ_r is the total probability of a fish taking route
200 *r*. Thus, S_r is the product of reach-specific survival probabilities that trace a unique migration
201 route through the Delta (e.g., $S_{\text{D}} = S_{\text{A2}} S_{\text{A3}} S_{\text{D4}} S_{\text{D5}}$), and Ψ_r is the product of routing probabilities
202 along that route (e.g., $\Psi_{\text{D}} = \Psi_{\text{AA3}} \Psi_{\text{AD4}}$, Perry et al., 2010).
203
204 *Time-varying individual covariates*
205 We hypothesized that river discharge affected migration routing, travel times, survival,
206 and detection probabilities. Mean daily discharge varies among the nine reaches owing to the
207 distribution of total discharge among the Delta's channel network. However, tidally averaged
208 net discharge in most reaches is a direct function of 1) river flows entering the Delta (as
209 measured in the Sacramento River at Freeport located near telemetry station A_2 in Fig. 1), and 2)
210 whether the Delta Cross Channel Gate is open or closed (Fig. S1; supplementary data are
211 available online). Furthermore, as river inflow increases, tidal fluctuations are dampened in all
212 but reaches 7 and 8 (Fig. 3). Therefore, we used river discharge at Freeport (Q) and the position
213 of the Delta Cross Channel gate (G = 1 or 0 for gates open or gates closed, respectively) as an
214 index of variation in reach-specific mean discharge affecting migration routing, travel times,
215 survival, and detection probabilities. Specifically, time-varying individual covariates Q_d and
216 G_d were assigned based on the day *d* when the *i*th individual passed a telemetry station in route
217 *r* at sampling occasion *j*.

We modeled μ, the log-mean of the travel time distribution, as a linear function of individual time-varying covariates:

$$\mu_{i,r,j} = \alpha_{0,r,j} + \alpha_{1,r,j} Q_d + \alpha_{2,r,j} G_d + z_{\mu,n,r,j} \xi_{\mu,r,j} \quad (2)$$

where r, j indexes the route and occasion where individuals entered reaches 0, …, 8 (Fig. 1 and 2), $\mu_{i,r,j}$ is the log-mean travel time for individual i in each reach, $\alpha_{0,r,j}$ is the intercept, $\alpha_{1,r,j}$ is the slope for the effect of discharge on μ, and $\alpha_{2,r,j}$ is the effect of Delta Cross Channel gate position on μ. We modeled $\sigma_{r,j}$, the variance parameter of the log-normal travel time distribution, as a constant for all individuals within a reach. In addition, $\alpha_{2,r,j}$ was set to zero for reaches located upstream of the of the Delta Cross Channel (i.e., for reaches 0, 1, 2, 3, and 6).

Given that discrete groups of fish were released in different months, years, and locations, we expected considerable variation in release-specific travel time, survival, and routing over and above variation that could be accounted for by covariates in the model. Extra variation among release groups was structured as a non-centered random effect where $z_{\mu,n,r,j}$ in Eq. 2 is a standard normal deviate for the nth release group entering each reach, $\xi_{\mu,r,j}$ is the standard deviation of the random effect in each reach, and their product is the deviation of each release group from the mean, conditional on the covariates. We used a non-centered random effect to reduce autocorrelation and speed convergence of the model fitting routine (Papaspiliopoulos et al. 2007; Monnahan et al. 2017).

Reach-specific survival was modeled as a logistic function using the same linear structure as travel time:

$$\text{logit}\left(S_{i,r,j}\right) = \beta_{0,r,j} + \beta_{1,r,j} Q_d + \beta_{2,r,j} G_d + \beta_3 \ell_i + z_{S,n,r,j} \xi_{S,r,j} \quad (3)$$

where logit(·) is the logit link function, ℓ_i is the fork length of individual *i*, β_3 is the slope for the effect of fork length on survival, and all other coefficients are defined as in Eq. 2 except with respect to survival. In this model, survival is constant among individuals that enter a given reach on a particular day. Travel time influences survival only through its effect on arrival times to a given telemetry station, which determines the discharge that individuals experienced when they entered a given reach.

We modeled three routing probabilities as a function of covariates: Ψ_{AB3}, Ψ_{AC4}, and $\Psi_{AD4|C'}$. Here, Ψ_{AB3} is the probability of entering Sutter and Steamboat Slough (route B) from the Sacramento River (route A) at sampling occasion 3, Ψ_{AC4} is the probability of entering the Delta Cross Channel (route C) from the Sacramento River at sampling occasion 4, and $\Psi_{AD4|C'}$ is the probability of entering Georgiana Slough (route D) from the Sacramento River, conditional on not having entered the Delta Cross Channel (C'). Since routing probabilities must sum to one at each of the two river junctions, the unconditional probability of entering Georgiana Slough (Ψ_{AD4}) at sampling occasion 4 is $\left(1-\Psi_{AC4}\right)\Psi_{AD4|C'}$.

We model routing probabilities using a generalized logistic function:

$$\Psi_i = L + \frac{U-L}{1+\exp\left(-\left(\gamma_0+\gamma_1 Q_d+\gamma_2 G_d+z_{\gamma,n}\xi_\Psi\right)\right)} \quad (4)$$

where Ψ_i is one of the three routing probabilities described above for individual *i*, *L* is the lower limit of Ψ_i, *U* is the upper limit of Ψ_i, and all other parameters are described as in Eq. 2 except with respect to routing. The parameters *U* and *L* allow the logistic function to take on values other than one or zero for upper and lower limits, respectively. This equation reduces to the standard inverse logit function by setting $U = 1$ and $L = 0$. We used the generalized logistic

function because we expected routing probabilities to follow a relationship similar to that between total discharge (Q) and the fraction of discharge entering each route. As these channels transition from bidirectional tidal flows to unidirectional flows with increasing total discharge, the fraction of discharge entering a route either increases (Sutter and Steamboat sloughs) or decreases (Georgiana Slough) with discharge before leveling off at a constant fraction of discharge (Fig. S2). Therefore, for Sutter and Steamboat Slough (Ψ_{AB3}) we set $L = 0$ and $\gamma_2 = 0$; for the Delta Cross Channel (Ψ_{AC4}) we set $L = 0$, $U = 1$, and $\gamma_2 = 0$; and for Georgiana Slough ($\Psi_{AD4|C'}$) we set $U = 1$.

We hypothesized that increases in discharge could reduce detection probabilities by increasing acoustic noise and by increasing the speed at which juvenile salmon pass telemetry stations. In addition, many telemetry stations were monitored each year with different hydrophones, varying numbers of hydrophones, and different spatial configurations that could have influenced detection probability. Therefore, we modeled these effects on detection probability as linear on the logit scale:

$$\text{logit}\left(P_{i,r,j}\right) = \theta_{0,r,j,y} + \theta_{1,r,j} Q_d \quad (5)$$

where $\theta_{0,r,j,y}$ is an intercept for year y at occasion j within route r, and $\theta_{1,r,j}$ is the slope for the effect of river discharge on detection probability at occasion j in route r.

Complete data likelihood

To estimate model parameters as a function of time-varying individual covariates, we used the complete data likelihood of the multistate model within a Bayesian framework. The complete data likelihood proceeds as if there were no missing values by augmenting the observed data with the unobserved missing data and treating the missing data as additional model

283 parameters to be estimated (King et al. 2010; Link and Barker 2010). This approach relies on
284 using an appropriate probability model for imputing missing covariate values and then
285 constructing the joint likelihood of the mark-recapture model parameters, the covariate model
286 parameters, and the missing data (Bonner and Schwarz 2004). To impute missing covariate
287 values for non-detected individuals whose arrival times are unknown, we model arrival times by
288 estimating parameters of the distribution of travel times through each reach.

289 The observed data for each individual required to estimate model parameters include 1)
290 the detection history, 2) cumulative travel times, 3) reach-specific travel times, and 4) covariates
291 linked to the fish's arrival time in each reach. A "detection history" is the alpha-numeric vector
292 h_i indicating whether individual *i* was detected in route *r* at occasion *j* ($h_{i,j}$ = A, B, C, or D) or
293 not detected at occasion *j* ($h_{i,j}$ = 0). The detection history compactly represents each fish's
294 detection and movement history through the telemetry network. For example, the detection
295 history A0ADD00 indicates a fish that was released into the Sacramento River ($h_{i,1}$ = A) and was
296 not detected at A_2 but was detected at A_3 ($h_{i,2:3}$ = 0A), indicating it remained in the Sacramento
297 River at its junction with Sutter and Steamboat sloughs. This fish was then detected entering
298 Georgiana Slough at D_4 and once more at D_5 before never being detected again ($h_{i,4:7}$ = DD00).
299 Associated with the observed detection history of each individual is the vector of observed
300 cumulative travel times T_i. For example, if h_i = A0ADD00 then T_i = ($T_{i,1}$, NA, $T_{i,3}$, $T_{i,4}$, $T_{i,5}$,
301 NA, NA) where $T_{i,1} = 0$, $T_{i,j}$ is the time from release to detection at a telemetry station at
302 sampling occasion *j*, and $T_{i,j}$ is missing (NA) when an individual is not detected. Time-varying
303 covariate values $x_{i,j}$ defined based on arrival date in each reach are missing (NA) whenever an
304 individual is not detected. Thus, for A0ADD00, x_i = ($x_{i,1}$, NA, $x_{i,3}$, $x_{i,4}$, $x_{i,5}$, NA, NA).

305 Observed reach-specific travel times $t_{i,r,j}$ for individual *i* in route *r* at occasion *j* are obtained by
306 taking the consecutive differences of the cumulative travel times. For A0ADD00, t_i = (NA, NA,
307 $t_{i,\mathrm{A3}}$, $t_{i,\mathrm{D4}}$, NA, NA). Note that $t_{i,r,j}$ is observed only when fish are detected at consecutive
308 telemetry stations whereas $T_{i,j}$ is defined whenever a fish is detected.

309 Adapting the notation of the King et al. (2010), the complete data likelihood augments
310 the observed detection history, h_i, by imputing the latent (unobserved) states when individuals
311 are not detected:

312 (6) $$z_{i,j} = \begin{cases} h_{i,j} & \text{if } h_{i,j} \neq 0 \\ g_{i,j} & \text{if } h_{i,j} = 0 \end{cases}$$

313 where $g_{i,j}$ is the latent state of unobserved individual *i* at detection occasion *j*, $z_{i,j}$ is the state of
314 individual *i* at detection occasion *j* (whether detected or non-detected), and z_i is the complete
315 state history for individual *i*. Although death can never be directly observed in detection history
316 h_i, death is included as a latent state such that $g_{i,j} \in (A, B, C, D, \dagger)$ where † is the death state.

317 The complete data likelihood is the product of three conditional likelihoods: 1) a
318 Bernoulli distribution for detection at occasion *j* given survival to occasion *j* in state *r*, 2) a
319 Bernoulli distribution for survival from occasion *j* to *j*+1 in state *r* given survival to occasion *j*,
320 and 3) a generalized Bernoulli distribution (i.e., a multinomial distribution for a single
321 observation) for the probability of moving from state *r* at occasion *j* to state *s* at occasion *j*+1
322 given survival to occasion *j*+1:

323 (7) $$L[S, \Psi, P \mid h, g] = \prod_{i=1}^{N} \prod_{j=F_i}^{J-1} \prod_{r \in R_j} \left[P_{i,r,j+1}^{u_{i,j+1,r}} \left(1 - P_{i,r,j+1}\right)^{v_{i,j+1,r}} \right] \left[S_{i,r,j}^{w_{i,j,r,}} \left(1 - S_{i,r,j}\right)^{w_{i,j,r,\dagger}} \right] \prod_{s \in R_{j+1}} \Psi_{i,r,s,j}^{w_{i,j,r,s}}$$

324 where

325 F_i is the occasion of release for individual *i*,

326 R_j is the set of states, excluding the death state, available to an individual in state *r* at occasion *j*

327 (Fig. 2),

328 $u_{i,j,r} = I\left(h_{i,j} = r\right)$ and $I(\cdot)$ is an indicator function resolving to one if individual *i* is detected in

329 state *r* at occasion *j* and zero otherwise,

330 $v_{i,j,r} = I\left(g_{i,j} = r\right)$ is one if individual *i* is imputed to be in state *r* at detection occasion *j* and zero

331 otherwise,

332 $w_{i,j,r,s} = I\left(z_{i,j} = r, z_{i,j+1} = s\right)$ is one if individual *i* is in state *r* at detection occasion *j* and in state *s*

333 at detection occasion *j*+1 and zero otherwise.

334 Note that $w_{i,j,r,\dagger}$ is one if individual *i* dies between *j* and *j*+1, $w_{i,j,r,\cdot} = \sum_{s \in R_{j+1}} w_{i,j,r,s}$ is one if the

335 individual survives, and the dot represents any state but the death state.

336 We modeled reach-specific travel times using a lognormal distribution because travel

337 times of migrating juvenile salmon are typically right-skewed, and the lognormal distribution

338 often fits travel time data well (Muthukumarana et al. 2008). Missing travel times (i.e., $t_{i,r,j}$ =

339 NA) are imputed from a lognormal distribution subject to the constraint

340 (8) $$T_{i,j+K} = T_{i,j} + \sum_{k=0}^{K-1} t_{i,r,j+k}^{\text{mis}}$$

341 where $T_{i,j}$ and $T_{i,j+K}$ are observed cumulative travel times, $t_{i,r,j}^{\text{mis}}$ are missing reach-specific travel

342 times between occasions *j* and *j*+*K*, and the *K* is the number of missing reach-specific travel

343 times between $T_{i,j}$ and $T_{i,j+K}$ (K = 2, …, J-1). Since the sum of missing travel times are

344 constrained to be equal to $T_{i,j+K} - T_{i,j}$, this constraint on imputed travel times imposes a form of
345 left censoring, thereby providing additional information to the parameter estimation.
346 Given observed and imputed travel times, the complete data likelihood for the travel time
347 data is:

348 (9) $$L\left[\mu,\sigma \mid t^{\text{obs}}, t^{\text{mis}}\right] \propto \prod_{i=1}^{N} \prod_{j=F_i}^{J-1} \prod_{r \in R_j} \frac{1}{\sigma_{i,r,j} t_{i,r,j}} \exp\left(\frac{-\left(\ln\left(t_{i,r,j}\right) - \mu_{i,r,j}\right)^2}{2\sigma_{i,r,j}^2} \right)$$

349 where $t_{i,r,j}$ is the observed (t^{obs}) or imputed (t^{mis}) travel time for individual *i* in state *r* at
350 detection occasion *j* and $\sigma_{i,r,j}^2$ is the variance of the lognormal travel time distribution for
351 individual *i* in state *r* at occasion *j*. We estimated $\sigma_{i,r,j}^2$ as a constant over all individuals for each
352 reach.
353
354 *Other parameter constraints*
355 In addition to constraining parameters as a function of covariates, a number of other
356 constraints were imposed owing to telemetry station outages, multiple release locations, and
357 parameter identifiability issues.
358 For reach 0, individuals were either released at Sacramento (rkm 172), at rkm 191, or
359 well upstream of these locations (>rkm 191, Table 1). For fish released well upstream of
360 Sacramento, we included in the analysis only those that were detected by telemetry stations in
361 the vicinity of Sacramento or at a telemetry station located near the Feather River at rkm 204
362 (see "number analyzed" in Table 1). To account for the effect of detection or release upstream of
363 Sacramento on travel times through reach 0, we included coefficients that estimated the

364 difference in intercepts for fish detected at rkm 204 or released at rkm 191 relative to those
365 detected or released at Sacramento (rkm 172).

366 We treated the first reach after release as an "acclimation" reach to allow fish to recover
367 from handling and release procedures before drawing inferences about travel time and survival
368 (reach 0 for releases at Sacramento and reach 5 for releases in Georgiana Slough). Therefore,
369 fish released directly into Georgiana Slough (rkm 115, Table 1) were modeled with unique
370 coefficient values in reach 5 relative to fish that entered reach 5 volitionally from upstream
371 locations. Coefficients based only on fish that entered reach 5 volitionally were then used for
372 inference about travel time and survival in reach 5.

373 Telemetry station A_3 was not deployed until January 2007, affecting release 1, and was
374 not deployed between December 2007 and March 2008, affecting releases 4–7. To incorporate
375 the effect of these receiver outages, detection probability was set to zero for fish that were
376 imputed to arrive at site A_3 during these time periods. In preliminary analysis, we found
377 coefficients associated with survival in reach 2 were weakly identifiable (i.e., large credible
378 intervals), and we identified undue influence of the prior distribution on U, the upper limit of the
379 logistic function for routing into Sutter and Steamboat Slough (Ψ_{AB3}). Both issues were likely
380 driven by the extended receiver outages at telemetry station A_3. Therefore, we set all survival
381 coefficients for reach 2 equal to those for reach 1 and estimated common slopes, intercepts, and
382 random-effects parameters. This constraint was supported by previous analyses showing similar
383 survival between reaches 1 and 2 (Perry 2010; Perry et al. 2010).

384 For routing into Sutter and Steamboat Slough, we included auxiliary data from an
385 independent telemetry study to bolster parameter estimates associated with Ψ_{AB3} (California
386 Department of Water Resources 2016, Romine et al. 2017). Of 4,528 acoustically tagged

387 juvenile late-fall Chinook salmon released at Sacramento between 1 March and 15 April 2014,
388 3,548 fish were detected at the junction of the Sacramento River and Sutter and Steamboat
389 Slough. We modeled this binary data (1 = Sutter and Steamboat Slough, 0 = Sacramento River)
390 using a Bernoulli likelihood with probability Ψ_{AB3} and jointly estimated the parameters of Eq. 4
391 for Ψ_{AB3} over both data sets.

392 Last, unique detection probabilities could not be estimated at the entrance to the Delta
393 Cross Channel (telemetry station C_4) and Georgiana Slough (telemetry station D_4) owing to a
394 single downstream detection site common to both reaches (telemetry station D_5). Therefore, a
395 common set of coefficients for detection probability were estimated for sites D_4 and C_4.
396
397 *Prior distributions, parameter estimation, and goodness of fit*

398 Prior distributions for parameters associated with routing, survival, and detection were
399 based on the default priors for logistic regression recommended by Gelman et al. (2013). First,
400 all continuous covariates were scaled to have mean zero and standard deviation 0.5 (for
401 discharge, Q, mean = 610.1 $m^3 \cdot s^{-1}$, SD = 407.1 $m^3 \cdot s^{-1}$; for fork length, ℓ, mean = 155.1 mm, SD
402 = 10.8 mm). Next, slope parameters associated with routing, survival, and detection were drawn
403 from a Student's t distribution with a mean of zero, standard deviation of 2.5, and 7 degrees of
404 freedom. Intercepts associated with routing, survival, and detection were drawn from a
405 Cauchy(0, 10) distribution. We used a Normal(0, 1) distribution truncated at zero as the prior
406 distribution for ξ_S and ξ_Ψ (Gelman et al. 2013). Last, a Uniform(0, 1) prior was used for L and
407 U. For travel time parameters, slopes and intercepts for μ were drawn from a Normal(0, 10)
408 prior distribution, and ξ_μ and σ were drawn from a Uniform(0, 10) prior.

We coded the model in the Markov Chain Monte Carlo (MCMC) software package JAGS (http://mcmc-jags.sourceforge.net/) as called from R (Denwood 2016), which allowed us to simultaneously estimate all model parameters and impute missing data (see Supplement B[1]). JAGS uses Gibbs sampling and Metropolis-Hastings methods to sequentially update each parameter value, conditional on the current value for all other parameters. We ran three MCMC chains in JAGS each for 50,000 iterations that consisted of a 1000-iteration adaptation phase and an additional 30,000-iteration burn-in phase. The final 20,000 iterations were thinned at a rate of 1 in 20 resulting in 1,000 iterations from each chain that were used to form the joint posterior distribution of the parameters. With these MCMC settings, the model took five days to run (10,000 iterations per day) on desktop computer with a 3.5 GHz processer and 64 GB of RAM.

We inspected trace plots of each MCMC chain and used the $\hat{R}$ statistic to assess convergence of the posterior for each parameter, where $\hat{R} < 1.1$ indicates convergence (Gelman et al. 2013). We then performed posterior predictive checks to assess goodness of fit by simulating replicated data from the joint posterior distribution. We used the joint log-likelihood of the capture histories (Eq. 7) and travel times (Eq. 9) as a goodness of fit statistic, which was calculated for both observed and replicated data for each draw in the joint posterior distribution. We calculated the probability that the observed data could have been generated by the model by calculating the proportion of times that the likelihood of the observed data was greater than that for replicated data. Often referred to as a Bayesian *p*-value, a probability >0.95 or <0.05 is typically taken as evidence of lack of fit (Gelman et al. 2013).

Results

The $\hat{R}$ statistics indicated that the Markov Chains converged to a stable stationary distribution. Of the 155 estimated parameters, $\hat{R}$ was less than 1.1 for all but one parameter ($\theta_{0,D4,4}$, the intercept for *P* at telemetry station D_4 in year 4), and its $\hat{R}$ was 1.115, just slightly higher than the standard cutoff value. In addition, we found no evidence of lack of fit; 54.4% of log-likelihood values for the observed data were greater than those for replicated data, indicating that the observed data were just as likely to have been generated by the model compared to replicated data that was known to have been generated by the model.

Daily inflow to the Delta varied widely over the study period, ranging from 193 $m^3 \cdot s^{-1}$ to 2,180 $m^3 \cdot s^{-1}$ (Fig. 3), which encompassed the 1st to 95th percentile of daily discharge in the 69-year flow record for the December through March migration period. Inflows influenced detection probabilities, travel time, survival, and routing. We found that discharge had a negative effect on detection probabilities at most telemetry stations, but the magnitude of the effect declined from the upper to lower Delta as tidal influence increased (Fig. S3). In general, detection probabilities were greater than 0.8 at most telemetry stations when flows were below 1,000 $m^3 \cdot s^{-1}$, but decreased at higher flows with the rate of decrease varying among years and telemetry stations (Fig. S4).

Most survival and travel time parameters associated with reach 6 (the Delta Cross Channel) exhibited wide credible intervals because only 6 release groups were released prior to mid-December when the Delta Cross Channel undergoes mandatory closures for fish protection (Fig. 4). Consequently, there was relatively little data from which to estimate the effects of river discharge on travel time and survival for reach 6.

For all other reaches, we found that median travel time was influenced by river flow. Posterior distributions for the effect of flow on travel time (α_1) were negative and credible

454 intervals excluded zero, indicating that increases in river flow reduced median travel times (Figs.
455 4 and 5). Credible intervals for the effect of the Delta Cross Channel on median travel time (α_2)
456 overlapped zero, with the exception of reach 7, indicating little evidence for an effect of an open
457 gate on travel time (Fig. 4). Credible intervals for the standard deviation of the release-group
458 random effects (ξ_μ) were well above zero, providing evidence that median travel times varied
459 among release groups after accounting for other effects in the model. At low inflows, median
460 travel times for tidal reaches (reaches 7 and 8) were considerably longer than other reaches (Fig.
461 5). Furthermore, at low flows, median travel times for reach 8 were about 2.5 times that of reach
462 7.

463 In contrast to travel time, survival was strongly related to river flow in just three of eight
464 reaches. In the upper two reaches, which exhibit the least tidal influence, the effect of flow (β_1)
465 was positive (Fig. 4) but the relative change in survival was small because survival was >0.90
466 over the range of observed discharge (Fig. 6). However, we estimated strong positive effects of
467 river flow in reaches 3-5 (Fig. 4); these reaches transition from bidirectional to unidirectional
468 flow as river discharge increases (Fig. 3 middle panel). Although discharge affected travel time
469 in the tidal reaches (reaches 7 and 8), the posterior distributions of β_1 were centered on zero for
470 these reaches and credible intervals were narrow, providing strong evidence of little relationship
471 between survival and discharge. We also found evidence that operation of the Delta Cross
472 Channel, which removes water from the Sacramento River, was associated with lower survival in
473 reaches of the Sacramento River downstream of the Delta Cross Channel (reaches 4 and 7). For
474 these reaches, posterior medians of β_2 were negative, and 75–90% of the posterior distribution
475 was less than zero (Fig. 4). Similar to findings with travel time, the posterior distributions for
476 standard deviations of random effects associated with survival were positive, indicating

477 additional release-to-release variation in survival over and above the effects of covariates
478 included in the model. Last, we also found a positive effect of fork length on survival (β_3,
479 median = 0.152, 90% credible interval = 0.062–0.243, Fig. S5).

480 Reach-specific flow-survival relationships revealed that survival increased sharply with
481 river flow in transitional reaches but not riverine or tidal reaches (Fig. 6). Survival in riverine
482 reaches (reaches 1 and 2) were high regardless of discharge, approaching 1 as flow increased. In
483 transitional reaches, median survival at the lowest flows was about 0.75 for reach 4 (Sacramento
484 River) and 0.5 for reach 3 (Sutter and Steamboat Slough) and reach 5 (Georgiana Slough). In
485 these reaches, survival increased sharply with river flow, approaching 1 as river flow exceeded
486 1,000 $m^3 \cdot s^{-1}$, which coincides with the transition from bidirectional to unidirectional flow (Fig. 3
487 middle panel). In tidal reaches, survival was not related to discharge, but median survival in
488 reach 7 (Sacramento River) was about twice that observed in reach 8 (interior Delta).

489 We found that routing probabilities (Fig. 7) followed a relationship similar to that
490 between total discharge (Q) and the fraction of discharge entering each route (Fig. S2), indicating
491 that the distribution of mean daily flow among channels is a key driver of migration routing (see
492 also Cavallo et al. 2015). As discharge increases, the probability of entering Sutter and
493 Steamboat Slough increased by 12 percentage points from about 0.23 to an estimated upper limit
494 (U) of 0.35 (Table 2, Fig. 7). In contrast, as flow increases, the probability of entering Georgiana
495 Slough (when the Delta Cross Channel gate is closed) decreased by 16 percentage points from
496 0.43 to an estimated lower limit (L) of 0.27 (Table 2, Fig. 7). For these routes, routing
497 probabilities approach upper and lower limits at an inflow of about 1,000 $m^3 \cdot s^{-1}$ (Fig. 7), the
498 point at which transitional reaches switch from bidirectional to unidirectional flows (Fig. 3
499 middle panel). We found little variation in routing probability among release groups for Sutter

and Steamboat Sloughs and the Delta Cross Channel, but considerable variation for Georgiana Slough, particularly at low discharge (Fig. 7).

We found that operation of the Delta Cross Channel increased the proportion of fish migrating through interior Delta (reach 8) where survival is low. Routing into the Delta Cross Channel decreased as flow increased, although credible intervals were wide (Table 2, Fig. 7). We found evidence that an open Delta Cross gate reduced the probability of entering Georgiana Slough (Table 2, Fig. 7 lower right panel). However, the combined probability of entering Georgiana Slough and Delta Cross Channel, both of which lead fish to the interior Delta (reach 8), was 15 percentage points higher than the probability of entering Georgiana Slough alone when the gates are closed (Fig. 7 lower right panel).

The reach-specific survival relationships with flow dictate the composite survival of juvenile salmon migrating through the Delta via alternative migration routes. At low flows, fish migrating through the Sacramento River exhibit the highest through-Delta survival, followed by Sutter and Steamboat Slough, but as river discharge increases, survival for Sutter and Steamboat Slough approaches that of the Sacramento River, leveling off at a survival of about 0.75 (Fig. 8). Survival of fish migrating through Georgiana Slough also increases with inflow but approaches a maximum of about 0.4. Since survival in all reaches except 7 and 8 approach 1 as discharge increases, survival in the tidal reaches imposes an upper limit on the overall through-Delta flow-survival relationship for each route.

Since routing probabilities determine the fraction of the population experiencing a given route-specific survival, both factors contribute to the shape of the relationship between overall survival and discharge. Mean overall survival increases with discharge from about 0.32 to 0.70 and falls in between the route-specific survival relationships (Fig. 8 lower right panel).

523 However, at low flows, overall survival is pulled more towards the low survival of Georgiana
524 Slough (Fig. 8 lower right panel) because the proportion of fish entering Georgiana Slough is
525 highest at low flows (Fig. 7). By contrast, as the proportion of fish entering Georgiana Slough
526 decreases with increasing flow, overall survival not only increases owing to the flow-survival
527 relationships, but is weighted more towards the higher-survival migration routes owing to the
528 flow-routing relationships.

529 Route-specific travel time distributions also vary considerably with river flow, and fish
530 traveling through the interior Delta (reach 8) via Georgiana Slough or the Delta Cross Chanel
531 exhibit longer travel times than those that migrate through the north Delta via the Sacramento
532 River and Sutter and Steamboat Slough (Fig. 9). For example, at inflows of 235 $m^3 \cdot s^{-1}$, the
533 median travel time for Georgiana Slough is 18.0 d, with some travel times as long as 40 d. By
534 comparison, for north Delta routes, median travel times are 12.2–12.6 d, with the tail of the
535 distribution extending to 30 d. In contrast, at inflows of 1,357 $m^3 \cdot s^{-1}$, expected median travel
536 times are 2.7–3.1 d for north Delta routes compared to 6.4 d for Georgiana Slough, with a 10-d
537 difference between the tails of the distributions.
538

539 **Discussion**

540 Understanding spatiotemporal variation in survival of migrating populations is critical for
541 identifying underlying mechanisms driving survival, particularly in a highly dynamic and
542 spatially complex environment such as the Sacramento-San Joaquin River Delta. Although
543 variation in survival of juvenile salmon migrating through the Delta has long been linked to
544 freshwater inflows (Kjelson and Brandes 1989; Newman and Rice 2002; Newman 2003), we
545 lacked understanding of how spatial variation in survival gave rise to this overall relationship.

Our analysis has revealed that the overall flow-survival relationship is driven by three key reaches that transition from unidirectional flow at high inflows to tidally driven bidirectional flow at low inflows. In contrast, riverine reaches exhibited high survival at all levels of inflow and tidal reaches had lower but constant survival with respect to inflow. Thus, the flow-survival relationship captures the gradient that occurs as transitional reaches shift from tidal to riverine environments as inflow increases.

In addition to being the hub of California's water delivery system, the Delta forms a critical nexus between freshwater and ocean environments. Juvenile salmon emigrating from natal tributaries first experience a tidal environment during their migration through the Delta. Juvenile salmon are particularly vulnerable during this transition because they must modify their migration tactics to progress seaward while undergoing physiological changes in preparation for seawater entry. Although some researchers have found high survival rates in estuaries (Clark et al. 2016), others have found that migration through estuaries is associated with high mortality rates relative to riverine or early marine phases (Thorstad et al. 2012 and references therein). For example, in a study of juvenile Atlantic salmon (*Salmo salar*) in riverine, estuarine, and early ocean environments, Halfyard et al. (2013) found that survival was most impacted in estuarine habitats near the head of tide. Our study is consistent with these findings and highlights how river inflows can interact with tides to influence survival by shifting the location at which the hydrodynamics switch from unidirectional to bidirectional flow.

Many studies (ours included) have correlated travel time and survival to river flow because these relationships provide a direct linkage between a key management variable and the subsequent response of migrating juvenile salmon populations (Connor et al. 2003; Smith et al. 2003; Courter et al. 2016). However, it is important to recognize that river flow affects travel

time and survival through both direct and indirect mechanisms. River flow directly influences migration rates of juvenile salmon by dictating water velocity, which is a function of channel geometry (Zabel and Anderson 1997; Zabel 2002; Tiffan et al. 2009). In turn, migration rates dictate arrival timing at ocean entry, which can influence early ocean survival (Satterthwaite et al. 2014). In contrast, river flow affects survival indirectly through a number of possible mechanisms. River flow can affect the proportion of fish using alternative routes at hydroelectric projects (Coutant and Whitney 2000) and in channel network systems such as the Delta (Cavallo et al. 2015; Perry et al. 2015). If survival differs among routes, which is often the case, then river discharge affects population survival by influencing the proportion of fish using high- or low-survival routes (Perry et al. 2013, 2016). In addition, river flow is often correlated with other environmental variables that influence survival such as turbidity and water temperature (Baker et al. 1995; Connor et al. 2003; Smith et al. 2003), which in turn may influence predation rates (Vogel and Beauchamp 1999; Ferrari et al. 2013).

Reducing travel time and exposure to predators is a key mechanism by which river flow has been hypothesized to affect survival of migrating juvenile salmonids, but establishing this linkage has proven elusive. Although travel time has been consistently linked with discharge via water velocity, some studies in the Snake and Columbia Rivers found no significant relationship between travel time and survival, but a significant relation between migration distance and survival (Bickford and Skalski 2000; Smith et al. 2002). To explain these counterintuitive findings, Anderson et al. (2005) developed a predator-prey model that expressed survival as a function of both travel time and travel distance. Their analysis revealed that the dependence of survival on travel time is dictated by the nature of predator-prey interactions. When prey migrate in a directed fashion through a field of stationary predators, survival is independent of travel time

592 and depends only on travel distance. In contrast, survival depends on travel time when random
593 movement dominates directed migration or when predators adopt prey searching tactics. These
594 findings illustrate how the relationship between flow and survival is context dependent, arising
595 from a combination of mechanisms that may directly affect survival (e.g., temperature) or
596 indirectly affect survival by modifying predator encounter rates (temperature, turbidity, predator
597 and prey behavior). Although our analysis here focused on estimating the association between
598 discharge and survival, our modeling framework allows exploration of alternative model
599 structures for linking flow to survival via travel time. For example, the XT model can be
600 incorporated into our analytical framework and compared against the current model structure to
601 assess the strength of evidence for the dependence of survival on travel time.

602 Predation by a host of non-native piscivorous fishes is thought to be the primary
603 proximate cause of juvenile salmon mortality in the Delta (Cavallo et al. 2013; Grossman 2016;
604 Sabal et al. 2016). Variation in survival among reaches observed in our study is consistent with
605 expectations based on predator-prey models. Juvenile salmon migrate downstream through
606 riverine reaches in a directed fashion and survival was high regardless of inflows and variation in
607 travel time. We observed a similar pattern at high flows when transitional reaches exhibit
608 unidirectional flows similar to riverine reaches. As inflow declines and tidal influence moves
609 upstream into transitional reaches, not only does travel time increase but travel distance increases
610 because juvenile salmon may be advected upstream on flood tides (Moser et al. 1991).
611 Simultaneously increasing both travel time and cumulative travel distance will act to increase
612 predator encounter rates. Thus, the flow-survival relationship that we observed in transitional
613 reaches likely arises from the transition from directed downstream movement at high flows to
614 less directed, bidirectional movement during low flows. In tidal reaches, our *a priori* expectation

was that neither travel time nor survival would be related to inflow because the magnitude of tidal flows (on the order of ±3,500 $m^3 \cdot s^{-1}$) swamps the signal of net inflow (Fig. 3 bottom panel). Although we observed no relation between survival and inflow in tidal reaches, we were surprised to find a strong effect of inflow on travel time, suggesting that survival may be decoupled from travel time in tidal reaches.

We included only inflow, DCC gate position, and fork length as covariates on reach-specific survival, but numerous other factors drive variation in survival. By casting our mark-recapture model in a hierarchical Bayesian framework and including a random effect on release group, we were able to quantify the magnitude of this variation but not its source. Seasonal and annual variation in reach-specific predator densities, environmental drivers (e.g., water temperature, turbidity), and spring-neap tidal cycles will act to modulate how travel time and survival respond to changes in inflow, thereby propagating variation among cohorts of juvenile salmon that experience a common set of flow conditions. Specifically, variation in survival among release groups was highest in tidal reaches and in transition reaches during low inflows, further suggesting that tidal cycles play an important role in driving variation in survival. For example, at a given inflow, cohorts migrating through the Delta during neap tides will experience lower-magnitude flood tides and first encounter bidirectional flows further downstream relative to cohorts migrating during spring tides. The high release-to-release variation in our study provides opportunity for future work to quantify how factors other than inflow influence survival in the Delta.

Our Bayesian mark-recapture model makes two important advances in the development of statistical mark-recapture models used to estimate survival of migrating juvenile salmonids. First, modeling individual covariates that vary through time is challenging owing to missing

638 covariate values for undetected individuals. Consequently, most approaches have ignored
639 within- and among-individual variation by averaging covariates over individuals within release
640 groups (Conner et al. 2003; Smith et al. 2003) or averaging covariates over space and time for
641 each individual (Stitch et al. 2015). In contrast, our model allows for individual covariates that
642 vary through space and time by incorporating an auxiliary model for travel times to impute
643 missing travel time, reach entry times, and covariates at the time of reach entry. Given the
644 considerable capital expense associated with conducting telemetry studies, our framework allows
645 the maximum amount of information to be extracted from telemetry data sets that typically have
646 small sample sizes. Second, our joint travel time and mark-recapture model explicitly considers
647 both migration and demographic processes under a single analytical framework. Thus, our
648 modeling framework opens the door to a number of useful extensions such as modeling survival
649 directly as a function of an individual's travel time (Muthukumarana et al. 2008) or by using an
650 event-time framework (e.g., Sparling et al. 2006; Zabel et al. 2014) where survival can be
651 modeled as a function of temporal variation in covariates during an individual's residence time
652 within a reach.

653 Our analysis provides insight into how water management decisions that influence inflow
654 and water routing are likely to affect travel time, routing, and survival of migrating juvenile
655 salmonids. First, survival decreases sharply and routing into the interior Delta (where survival is
656 low) increases sharply as Delta inflows decline below approximately 1,000 $m^3 \cdot s^{-1}$, the point at
657 which transitional reaches shift from bidirectional to unidirectional flow (Figs 7 and 8). In
658 contrast, at inflows greater than 1,000 $m^3 \cdot s^{-1}$, survival is maximized and changes relatively little
659 with flow while routing into the interior Delta via Georgiana Slough is minimized and insensitive
660 to inflow. These findings indicate that water management actions that reduce inflows to the Delta

will have relatively little effect on survival at high flows, but potentially considerable negative effects at low flows. Furthermore, operation of the Delta Cross Channel not only increases the fraction of the population that enters the interior Delta where survival is low (Fig. 7), but is associated with lower survival for the Sacramento River (Fig. 4). These compounding effects of opening the Delta Cross Channel act to further reduce overall survival relative to inflows alone (Fig. S6). Our findings illustrate how tradeoffs between juvenile salmon survival and water management for human use vary with the amount of flow entering the Delta. Thus, our modeling framework can be used as a management tool to explore the consequences of such tradeoffs and to quantitatively assess the effect of alternative management scenarios on travel time, routing, and survival.

Water flow has been dubbed the "master" variable in the Delta because of its economic importance and its pervasive effect on all components of this complex and dynamic aquatic ecosystem (Mount et al. 2012; Lund et al. 2015). Indeed, our work is beginning to shed light on the multiple ways in which river flows differentially affect survival in different reaches of the Delta and interact with water and fish routing to affect overall survival. In turn, these insights will aid managers in devising strategies to balance consumptive water use with management actions that aim to recover threatened and endangered salmon populations in the Sacramento River.

Acknowledgements

Funding for this study was provided by the Delta Stewardship Council, Grant 2045 (RWP and PLB, principal investigators). We are grateful to the many field biologists who helped to collect the data upon which our analysis was based. Special thanks to the staff of the Coleman National

684 Fish Hatchery for logistical support and for providing the juvenile salmon used in our analysis.
685 Amy Hansen, Ken Tiffan, and Josh Korman provided many insightful comments that improved
686 the manuscript. Any use of trade, firm, or product names is for descriptive purposes only and
687 does not imply endorsement by the U.S. Government

688

689 **References**

690 Anderson, J.J., Gurarie, E. and Zabel, R.W. 2005. Mean free-path length theory of predator–prey
691 interactions: application to juvenile salmon migration. Ecol. Modell. **186**(2): 196–211.
692 doi: 10.1016/j.ecolmodel.2005.01.014.

693 Baker, P.F., Ligon, F.K. and Speed, T.P. 1995. Estimating the influence of temperature on the
694 survival of Chinook salmon smolts (Oncorhynchus tshawytscha) migrating through the
695 Sacramento–San Joaquin River Delta of California. Can. J. Fish. Aquat. Sci. **52**(4): 855–
696 863. doi: 10.1139/f95-085.

697 Bickford, S.A. and Skalski, J.R. 2000. Reanalysis and interpretation of 25 years of Snake–
698 Columbia River juvenile salmonid survival studies. N. Am. J. Fish. Manage. **20**(1): 53–
699 68. doi: 10.1577/1548-8675(2000)020<0053:RAIOYO>2.0.CO;2.

700 Bonner, S.J. and Schwarz, C.J. 2004. Continuous time–dependent individual covariates and the
701 Cormack–Jolly–Seber model. Anim. Biodiversity Conserv. **27**(1): 49–155.

702 Brandes, P.L., and McLain, J.S. 2001. Juvenile Chinook salmon abundance, distribution, and
703 survival in the Sacramento–San Joaquin Estuary. *In* Contributions to the Biology of the
704 Central Valley Salmonids, Fish Bulletin 179, vol. 2. *Edited by* R.L. Brown. California
705 Department of Fish and Game, Sacramento, C.A. pp 39–138.

California Department of Water Resources. 2016. 2014 Georgiana Slough Floating Fish Guidance Structure Performance Evaluation Project Report. Bay-Delta Office, Sacramento, California. Available from http://baydeltaoffice.water.ca.gov/sdb/GS/docs/Final%20Report%20October%202016%20Edition%20103116-signed.pdf [accessed 22 November 2017].

Catchpole, E.A., Morgan, B.J. and Tavecchia, G. 2008. A new method for analysing discrete life history data with missing covariate values. J. R. Stat. Soc. B. **70**(2): 445–460. doi: 10.1111/j.1467-9868.2007.00644.x.

Cavallo, B., Merz, J. and Setka, J. 2013. Effects of predator and flow manipulation on Chinook salmon (*Oncorhynchus tshawytscha*) survival in an imperiled estuary. Environ. Biol. Fishes, **96**(2-3): 393–403. doi: 10.1007/s10641-012-9993-5.

Cavallo, B., Gaskill, P., Melgo, J. and Zeug, S.C. 2015. Predicting juvenile Chinook Salmon routing in riverine and tidal channels of a freshwater estuary. Environ. Biol. Fishes, **98**(6): 1571–1582. doi: 10.1007/s10641-015-0383-7.

Clark, T.D., Furey, N.B., Rechisky, E.L., Gale, M.K., Jeffries, K.M., Porter, A.D., Casselman, M.T., Lotto, A.G., Patterson, D.A., Cooke, S.J. and Farrell, A.P. 2016. Tracking wild sockeye salmon smolts to the ocean reveals distinct regions of nocturnal movement and high mortality. Ecol. App. **26**(4): 959–978. doi: 10.1890/15-0632.

Connor, W.P., Burge, H.L., Yearsley, J.R. and Bjornn, T.C. 2003. Influence of flow and temperature on survival of wild subyearling fall Chinook salmon in the Snake River. N.

726 Am. J. Fish. Manage. **23**(2): 362–375. doi: 10.1577/1548-
727 8675(2003)023<0362:IOFATO>2.0.CO;2.

728 Courter, I.I., Garrison, T.M., Kock, T.J., Perry, R.W., Child, D.B. and Hubble, J.D. 2016.
729 Benefits of prescribed flows for salmon smolt survival enhancement vary longitudinally
730 in a highly managed river system. River Res. Appl. **32**(10): 1999–2008. doi:
731 10.1002/rra.3066.

732 Coutant, C.C. and Whitney, R.R. 2000. Fish behavior in relation to passage through hydropower
733 turbines: a review. Trans. Am. Fish. Soc. **129**(2): 351–380. doi: 10.1577/1548-
734 8659(2000)129<0351:FBIRTP>2.0.CO;2.

735 Denwood, M.J. 2016. runjags: An R package providing interface utilities, model templates,
736 parallel computing methods and additional distributions for MCMC models in JAGS. J.
737 Stat. Software, **71**(9): 1–25. doi: 10.18637/jss.v071.i09.

738 Ferrari, M.C., Ranåker, L., Weinersmith, K.L., Young, M.J., Sih, A. and Conrad, J.L. 2013.
739 Effects of turbidity and an invasive waterweed on predation by introduced largemouth
740 bass. Environ. Biol. Fishes, **97**(1): 79–90. doi: 10.1007/s10641-013-0125-7.

741 Gelman, A., Carlin, J.B., Stern, H.S., Dunson, D.B., Vehtari, A. and Rubin, D.B. 2013. Bayesian
742 data analysis. CRC Press, Boca Raton, F.L.

743 Gibson, A.J.F., Halfyard, E.A., Bradford, R.G., Stokesbury, M.J. and Redden, A.M. 2015.
744 Effects of predation on telemetry-based survival estimates: insights from a study on
745 endangered Atlantic salmon smolts. Can. J. Fish. Aquat. Sci. **72**(5): 728–741. doi:
746 10.1139/cjfas-2014-0245.

747 Grossman, G.D. 2016. Predation on fishes in the Sacramento–San Joaquin Delta: current
748 knowledge and future directions. San Francisco Estuary and Watershed Science, **14**(2).
749 Available from http://escholarship.org/uc/item/9rw9b5tj [accessed 12 July 2017].

750 Halfyard, E.A., Gibson, A.J.F., Stokesbury, M.J., Ruzzante, D.E. and Whoriskey, F.G. 2013.
751 Correlates of estuarine survival of Atlantic salmon postsmolts from the Southern Upland,
752 Nova Scotia, Canada. Can. J. Fish. Aquat. Sci. **70**(3): 452–460. doi: 10.1139/cjfas-2012-
753 0287.

754 Healey, M., Goodwin, P., Dettinger, M., and Norgaard, R. 2016. The State of Bay–Delta Science
755 2016: An Introduction. San Francisco Estuary and Watershed Science, **14**(2). Available
756 from http://escholarship.org/uc/item/9k43h252. doi:
757 http://dx.doi.org/10.15447/sfews.2016v14iss2art5 [accessed 12 July 2017].

758 King, R., Morgan, B., Gimenez, O. and Brooks, S. 2010. Bayesian analysis for population
759 ecology. CRC press, Boca Raton, F.L.

760 Kjelson, M.A., Raquel, P.F., and Fisher, F.W. 1982. Life history of fall-run juvenile Chinook
761 salmon, *Oncorhynchus tshawytscha*, in the Sacramento–San Joaquin Estuary, California.
762 *In* Estuarine Comparisons. *Edited by* V.S. Kennedy. Academic Press, New York, N.Y.
763 pp. 393–411.

764 Kjelson, M.A. and Brandes, P.L. 1989. The use of smolt survival estimates to quantify the effects
765 of habitat changes on salmonid stocks in the Sacramento-San Joaquin rivers, California.
766 *In* Proceedings of the National Workshop on Effects of Habitat Alteration on Salmonid

767 Stocks, Nanaimo, B.C., 6–8 May 1987. Canadian special publication of fisheries and
768 aquatic sciences 105, Department of Fisheries and Oceans, Ottowa, Canada. pp. 100–115.

769 Link, W.A. and Barker, R.J. 2010. Bayesian inference: with ecological applications. Academic
770 Press, San Diego, C.A.

771 Lund, B., Brandt, S., Collier, T., Atwater, B., Canuel, E., Fernando, H.J.S., Meyer, J., Norgaard,
772 R., Resh, V., Wiens, J., and Zedler, J. 2015. Flows and fishes in the Sacramento-San
773 Joaquin Delta: Research needs in support of adaptive management. Delta Stewardship
774 Council, Sacramento, C.A. Available from
775 http://deltacouncil.ca.gov/sites/default/files/2015/09/2015-9-29-15-0929-Final-Fishes-
776 and-Flows-in-the-Delta.pdf [accessed 12 July 2017].

777 Michel, C.J., Ammann, A.J., Lindley, S.T., Sandstrom, P.T., Chapman, E.D., Thomas, M.J.,
778 Singer, G.P., Klimley, A.P. and MacFarlane, R.B. 2015. Chinook salmon outmigration
779 survival in wet and dry years in California's Sacramento River. Can. J. Fish. Aquat. Sci.
780 **72**(11): 1749–1759. doi: 10.1139/cjfas-2014-0528.

781 Monnahan, C.C., Thorson, J.T. and Branch, T.A. 2017. Faster estimation of Bayesian models in
782 ecology using Hamiltonian Monte Carlo. Methods Ecol. Evol. **8**(3): 339–348. doi:
783 10.1111/2041-210X.12681.

784 Moser, M.L., Olson, A.F. and Quinn, T.P. 1991. Riverine and estuarine migratory behavior of
785 coho salmon (*Oncorhynchus kisutch*) smolts. Can. J. Fish. Aquat. Sci. **48**(9): 1670-1678.
786 doi: 10.1139/f91-198.

787 Mount, J., Bennett, W., Durand, J., Fleenor, W., Hanak, E., Lund, J. and Moyle, P. 2012. Aquatic
788 Ecosystem Stressors in the Sacramento-San Joaquin Delta. Public Policy Institute of
789 California, San Francisco, C.A. Available from
790 http://www.ppic.org/content/pubs/report/R_612JMR.pdf [accessed 12 July 2017].

791 Muthukumarana, S., Schwarz, C.J. and Swartz, T.B. 2008. Bayesian analysis of mark-recapture
792 data with travel time-dependent survival probabilities. Can. J. Stat. **36**(1): 5–21. doi:
793 10.1002/cjs.5550360103.

794 Newman, K.B. 2003. Modelling paired release-recovery data in the presence of survival and
795 capture heterogeneity with application to marked juvenile salmon. Stat. Modell. **3**(3):
796 157–177. doi: https://doi.org/10.1191/1471082X03st055oa.

797 Newman, K.B. and Rice, J. 2002. Modeling the survival of Chinook salmon smolts outmigrating
798 through the lower Sacramento River system. J. Am. Stat. Assoc. **97**(460): 983-993. doi:
799 10.1198/016214502388618771.

800 Newman, K.B. and Brandes, P.L. 2010. Hierarchical modeling of juvenile Chinook salmon
801 survival as a function of Sacramento–San Joaquin Delta water exports. N. Am. J. Fish.
802 Manage. **30**(1): 157–169. doi: 10.1577/M07-188.1.

803 Papaspiliopoulos, O., Roberts, G.O. and Sköld, M. 2007. A general framework for the
804 parametrization of hierarchical models. Stat. Sci. **22**(1): 59–73.
805 doi:10.1214/088342307000000014.

806 Perry, R.W. 2010. Survival and migration dynamics of juvenile Chinook salmon (*Oncorhynchus*
807 *tshawytscha*) in the Sacramento-San Joaquin River Delta. Ph.D. dissertation, School of
808 Aquatic and Fishery Sciences, University of Washington, Seattle, W.A.

809 Perry, R.W., Skalski, J.R., Brandes, P.L., Sandstrom, P.T., Klimley, A.P., Ammann, A. and
810 MacFarlane, B. 2010. Estimating survival and migration route probabilities of juvenile
811 Chinook salmon in the Sacramento–San Joaquin River Delta. N. Am. J. Fish. Manage.
812 **30**(1): 142–156. doi: 10.1577/M08-200.1.

813 Perry, R.W., Romine, J.G., Brewer, S.J., LaCivita, P.E., Brostoff, W.N. and Chapman, E.D.
814 2012. Survival and migration route probabilities of juvenile Chinook salmon in the
815 Sacramento-San Joaquin River Delta during the winter of 2009-10. US Geological
816 Survey Open File Report No. 2012-1200. Available from
817 https://pubs.usgs.gov/of/2012/1200/ [accessed 12 July 2017].

818 Perry, R.W., Brandes, P.L., Burau, J.R., Klimley, A.P., MacFarlane, B., Michel, C. and Skalski,
819 J.R. 2013. Sensitivity of survival to migration routes used by juvenile Chinook salmon to
820 negotiate the Sacramento-San Joaquin River Delta. Environ. Biol. Fishes, **96**(2-3): 381–
821 392. doi: 10.1007/s10641-012-9984-6.

822 Perry, R.W., Brandes, P.L., Burau, J.R., Sandstrom, P.T. and Skalski, J.R. 2015. Effect of tides,
823 river flow, and gate operations on entrainment of juvenile salmon into the Interior
824 Sacramento–San Joaquin River delta. Trans. Am. Fish. Soc. **144**(3): 445–455. doi:
825 10.1080/00028487.2014.1001038 .

826 Perry, R.W., Buchanan, R.A., Brandes, P.L., Burau, J.R. and Israel, J.A. 2016. Anadromous
827 salmonids in the Delta: new science 2006–2016. San Francisco Estuary and Watershed
828 Science, **14**(2). Available from http://escholarship.org/uc/item/27f0s5kh [accessed 12
829 July 2017].

830 R Core Team. 2015. R: A language and environment for statistical computing. R Foundation for
831 Statistical Computing, Vienna, Austria. Available from https://www.R-project.org/
832 [accessed 20 October 2017].

833 Raymond, H.L. 1988. Effects of hydroelectric development and fisheries enhancement on spring
834 and summer chinook salmon and steelhead in the Columbia River basin. N. Am. J. Fish.
835 Manage. **8**(1): 1–24. doi: 10.1577/1548-8675(1988)008<0001:EOHDAF>2.3.CO;2.

836 Romine, J.G., Perry, R.W., Pope, A.C., Stumpner, P., Liedtke, T.L., Kumagai, K.K. and Reeves,
837 R.L. 2017. Evaluation of a floating fish guidance structure at a hydrodynamically
838 complex river junction in the Sacramento–San Joaquin River Delta, California, USA.
839 Marine and Freshwater Research, **68**(5): 878–888. doi: 10.1071/MF15285.

840 Sabal, M., Hayes, S., Merz, J. and Setka, J. 2016. Habitat alterations and a nonnative predator,
841 the Striped Bass, increase native Chinook Salmon mortality in the Central Valley,
842 California. N. Am. J. Fish. Manage. **36**(2): 309–320. doi:
843 10.1080/02755947.2015.1121938.

844 Satterthwaite, W.H., Carlson, S.M., Allen-Moran, S.D., Vincenzi, S., Bograd, S.J. and Wells,
845 B.K. 2014. Match-mismatch dynamics and the relationship between ocean-entry timing

and relative ocean recoveries of Central Valley fall run Chinook salmon. Mar. Ecol. Prog. Series. **511**: 237–248. doi. 10.3354/meps10934.

Skalski, J.R., Townsend, R., Lady, J., Giorgi, A.E., Stevenson, J.R., and McDonald, R.D. 2002. Estimating route-specific passage and survival probabilities at a hydroelectric project from smolt radiotelemetry studies. Can. J. Fish. Aquat. Sci. **59**(8): 1385–1393. doi: 10.1139/f02-094.

Smith, S.G., Muir, W.D., Williams, J.G. and Skalski, J.R. 2002. Factors associated with travel time and survival of migrant yearling Chinook salmon and steelhead in the lower Snake River. N. Am. J. Fish. Manage. **22**(2): 385–405. doi: 10.1577/1548-8675(2002)022<0385:FAWTTA>2.0.CO;2.

Smith, S.G., Muir, W.D., Hockersmith, E.E., Zabel, R.W., Graves, R.J., Ross, C.V., Connor, W.P. and Arnsberg, B.D. 2003. Influence of river conditions on survival and travel time of Snake River subyearling fall Chinook salmon. N. Am. J. Fish. Manage. **23**(3): 939–961. doi: 10.1577/M02-039.

Sparling, Y.H., Younes, N., Lachin, J.M. and Bautista, O.M. 2006. Parametric survival models for interval-censored data with time-dependent covariates. Biostatistics, **7**(4): 599–614. doi: https://doi.org/10.1093/biostatistics/kxj028.

Stich, D.S., Bailey, M.M., Holbrook, C.M., Kinnison, M.T. and Zydlewski, J.D. 2015. Catchment-wide survival of wild-and hatchery-reared Atlantic salmon smolts in a changing system. Can. J. Fish. Aquat. Sci. **72**(9): 1352–1365. doi: 10.1139/cjfas-2014-0573.

867 Thorstad, E.B., Whoriskey, F., Uglem, I., Moore, A., Rikardsen, A.H. and Finstad, B. 2012. A
868 critical life stage of the Atlantic salmon Salmo salar: behaviour and survival during the
869 smolt and initial post-smolt migration. J. Fish Biol. **81**(2): 500–542. doi: 10.1111/j.1095-
870 8649.2012.03370.x.

871 Tiffan, K.F., Kock, T.J., Haskell, C.A., Connor, W.P. and Steinhorst, R.K. 2009. Water velocity,
872 turbulence, and migration rate of subyearling fall Chinook salmon in the free-flowing and
873 impounded Snake River. Trans. Am. Fish. Soc. **138**(2): 373–384. doi: 10.1577/T08-
874 051.1.

875 Vogel, J.L. and Beauchamp, D.A. 1999. Effects of light, prey size, and turbidity on reaction
876 distances of lake trout (*Salvelinus namaycush*) to salmonid prey. Can. J. Fish. Aquat. Sci.
877 **56**(7): 1293–1297. doi: 10.1139/f99-071.

878 Ward Jr, J.H. 1963. Hierarchical grouping to optimize an objective function. J. Am. Stat. Assoc.
879 **58**(301): 236–244. doi: 10.1080/01621459.1963.10500845.

880 White, G.C. and Burnham, K.P. 1999. Program MARK: survival estimation from populations of
881 marked animals. Bird Study, **46**(sup1): S120–S139. doi: 10.1080/00063659909477239.

882 Zabel, R.W. 2002. Using "travel time" data to characterize the behavior of migrating animals.
883 Am. Nat. **159**(4): 372–387. doi: 10.1086/338993.

884 Zabel, R.W. and Anderson, J.J. 1997. A model of the travel time of migrating juvenile salmon,
885 with an application to Snake River spring chinook salmon. N. Am. J. Fish. Manage.
886 **17**(1): 93–100. doi: 10.1577/1548-8675(1997)017<0093:AMOTTT>2.3.CO;2.

887 Zabel, R.W., Burke, B.J., Moser, M.L. and Caudill, C.C. 2014. Modeling temporal phenomena in
888 variable environments with parametric models: an application to migrating salmon. Ecol.
889 Modell. **273**: 23–30.

890 **Tables**

891 **Table 1**. Description of release groups and data sources.

Release group	Source	Year	Release dates	Number released	Number analyzed	Release sites (rkm)
1	Perry et al. (2010, 2013)	2006	Dec 5-6	64	64	172
2	Perry et al. (2010, 2013)	2007	Jan 17-18	80	80	172
3	Michel et al. (2015)		Jan 15-Feb 2	200	11	517
4	Perry et al. (2013)		Dec 4-7	208	208	115, 172
5	Michel et al. (2015)		Dec 7	150	60	345, 398, 500
6	Perry et al. (2013)	2008	Jan 15-18	211	211	115, 172
7	Michel et al. (2015)		Jan 17	154	65	345, 398, 500
8	Perry et al. (2013)		Nov 30-Dec 6	292	292	115, 172
9	Michel et al. (2015)		Dec 13	149	82	345, 398, 500
10	Michel et al.	2009	Jan 11	151	63	345, 398, 500

	(2015)					
11	Perry et al. (2013)		Jan 13-19	292	292	115, 172
12	Perry et al. (2012)		Dec 2-5	239	239	115, 191
13	Michel et al. (2015)		Dec 15	153	63	345, 398, 500
14	Perry et al. (2012)		Dec 16-19	240	240	115, 191
15	Michel et al. (2015)	2010	Jan 6	153	42	345, 398, 500
16	Michel et al. (2015)		Dec 17	120	79	500
17	Michel et al. (2015)	2011	Jan 5	120	79	500
All groups				2,976	2,170	

892 **Note**: Release sites are indicated by river kilometer (rkm) measured from the distance to the
893 Pacific Ocean. For fish release upstream of the Delta (> rkm 208), the number analyzed
894 indicates fish that were included in the analysis based on detections at telemetry stations near the
895 entrance to the Delta at rkm 189 or rkm 226.
896

897 **Table 2.** Posterior medians (90% credible intervals) for routing probabilities expressed as a
898 function of time-varying individual covariates. Parameter values without associated credible
899 intervals were set to the given value.

Parameter	Sutter and Steamboat Slough (Ψ_{AB3})	Delta Cross Channel (Ψ_{AC4})	Georgiana Slough ($\Psi_{AD4\|C'}$)
U	0.35 (0.31 – 0.43)	1	1
L	0	0	0.27 (0.20 – 0.32)
γ_0	1.89 (0.91 – 3.30)	-1.49 (-2.40 – -0.67)	-2.95 (-4.57 – -1.83)
γ_1	2.17 (1.10 – 4.15)	-1.25 (-3.47 – 0.90)	-6.53 (-5.46 – -1.24)
γ_2	0	0	-0.55 (-2.76 – 0.33)
ξ_Ψ	0.19 (0.04 – 0.50)	0.31 (0.06 – 0.87)	0.89 (0.46 – 1.58)

900 **Note**: U = upper limit of logistic function, L = lower limit of logistic function, γ_0 = intercept, γ_1
901 = slope for effect of discharge on routing, γ_2 = slope for effect of open Delta Cross Channel
902 gates on routing, ξ_Ψ = standard deviation of the release group random effect.

903

Figure Captions

Fig. 1. Map of the Sacramento-San Joaquin River Delta showing the location of acoustic telemetry receiving stations (filled black circles) used to detect acoustic tagged juvenile salmon as they migrated through the Delta. Telemetry stations are labeled by migration route (A-D) and sampling occasion (1-7; see Fig. 2). These telemetry stations divide the Delta into eight discrete reaches (shown by numbered shaded regions), with an additional reach upstream of telemetry station A_2 (Reach 0) used as acclimation reach to allow fish to recover from post-release handling. The location of water pumping stations in the southern interior Delta is indicated by the pink diamonds. Data and maps copyright © 1999-2006 ESRI.

Fig. 2. Schematic of the multistate mark-recapture model with parameters indexed by state (migration route) and sampling occasion. Parameters include reach-specific survival probabilities (S), site-specific detection probabilities (P), routing probabilities (Ψ), and λ, the joint probability of surviving and being detected at telemetry stations downstream of site A_6. Release locations are indicated by the nth release in route r at occasion j: n_{A1} (at Sacramento or upstream – see Table 1) and n_{D4} in Georgiana Slough.

Fig. 3. Daily inflow into the Sacramento-San Joaquin River Delta (top panel) and tidal influence on discharge at three locations in the Sacramento River during 2010 (middle and bottom panels). The top panel shows mean daily discharge of the Sacramento River at Freeport (A_2 in Fig. 1). In the two lower panels, lines show mean daily discharge and the shaded regions encompass the daily minimum and maximum discharge with values less than zero indicating reverse flows

caused by tidal forcing. The middle panel shows the Sacramento River at Freeport (black line, gray shading) and the Sacramento River just downstream of Georgiana Slough (pink link and shading; A_4 in Fig. 1). The bottom panel shows the Sacramento River at Rio Vista (A_5 in Fig. 1).

Fig. 4. Summary of posterior distributions of parameters estimating the effects of river flow and Delta Cross Channel (DCC) gate position on travel time and survival. Points show the median of the posterior distribution, heavy lines show the 25th to 75th percentile, and thin lines show the 5th to 95th percentile. Green bars are density strips with darker regions illustrating higher posterior density. Parameter definitions as follows: α_1 = slope for effect of discharge on mean of log-travel time, α_2 = slope for effect of an open DCC gate on mean of log-travel time, ξ_μ = standard deviation of release group random effect on μ, σ = variance parameter of the lognormal travel time distribution, β_1 = slope for effect of discharge on survival, β_2 = slope for effect of an open DCC gate on survival, ξ_S = standard deviation of release group random effect on survival.

Fig. 5. Reach-specific relationships between median travel time and inflow to the Delta as measured at the Sacramento River at Freeport (shown for closed Delta Cross Channel gates and plotted at the mean fork length). The heavy magenta line shows the mean relationship and the dotted lines show the random effects estimates for each release group based on medians of the joint posterior distribution. The dark gray region shows 95% credible intervals about the mean relationship. The light gray region shows the 95% confidence interval among release groups.

Fig. 6. Reach-specific relationships between survival and inflow to the Delta as measured at the Sacramento River at Freeport (shown for closed Delta Cross Channel gates and plotted at the

mean fork length). The heavy magenta line shows the mean relationship and dotted lines show the random effects estimates for each release group based on medians of the joint posterior distribution. The dark gray region shows 95% credible intervals about the mean relationship. The light gray region shows the 95% confidence interval among release groups.

Fig. 7. Relationships between routing probability and inflow to the Delta as measured at the Sacramento River at Freeport (A_2 in Fig. 1). The lower right panel shows the effect of Delta Cross Channel (DCC) gate position on routing probabilities at the junction of the Sacramento River, Delta Cross Channel, and Georgiana Slough (A_4, C_4, and D_4 in Fig. 1), plotted at the posterior median of the parameters. Other panels show mean routing relationships (heavy magenta line), random effects estimates for each release group (dotted lines), 95% credible interval about the mean relationship (dark gray region), and 95% confidence interval among release groups (light gray region).

Fig. 8. Route-specific survival through the Sacramento-San Joaquin River Delta between Freeport (A_2 in Fig. 1) and Chipps Island (A_6 in Fig. 1). Route-specific survival based on posterior median parameter values was calculated as the product of reach-specific survival for reaches that trace each unique migration route through the Delta (shown for closed Delta Cross Channel gates). The first three panels show the mean relationship for each route with thin gray lines showing the random effects estimates for each release group. The last panel shows overall survival through Delta for all routes (with random effects estimates as thin gray lines) along with route-specific survival relationships. Overall survival was calculated as the average of route-specific survival weighted by routing probabilities (see Eq. 1).

973

974 **Fig. 9.** Route-specific travel time distributions between Freeport (A_2 in Fig. 1) and Chipps Island
975 (A_6 in Fig. 1) at the 5th (top panel) and 95th (bottom panel) percentiles of discharge based on the
976 historical flow record (235 $m^3 \cdot s^{-1}$ and 1357 $m^3 \cdot s^{-1}$, respectively). Arrows show the median travel
977 times for each route. Travel time distributions were based on posterior medians of parameters
978 for reach-specific travel time distributions assuming closed Delta Cross Channel gates.

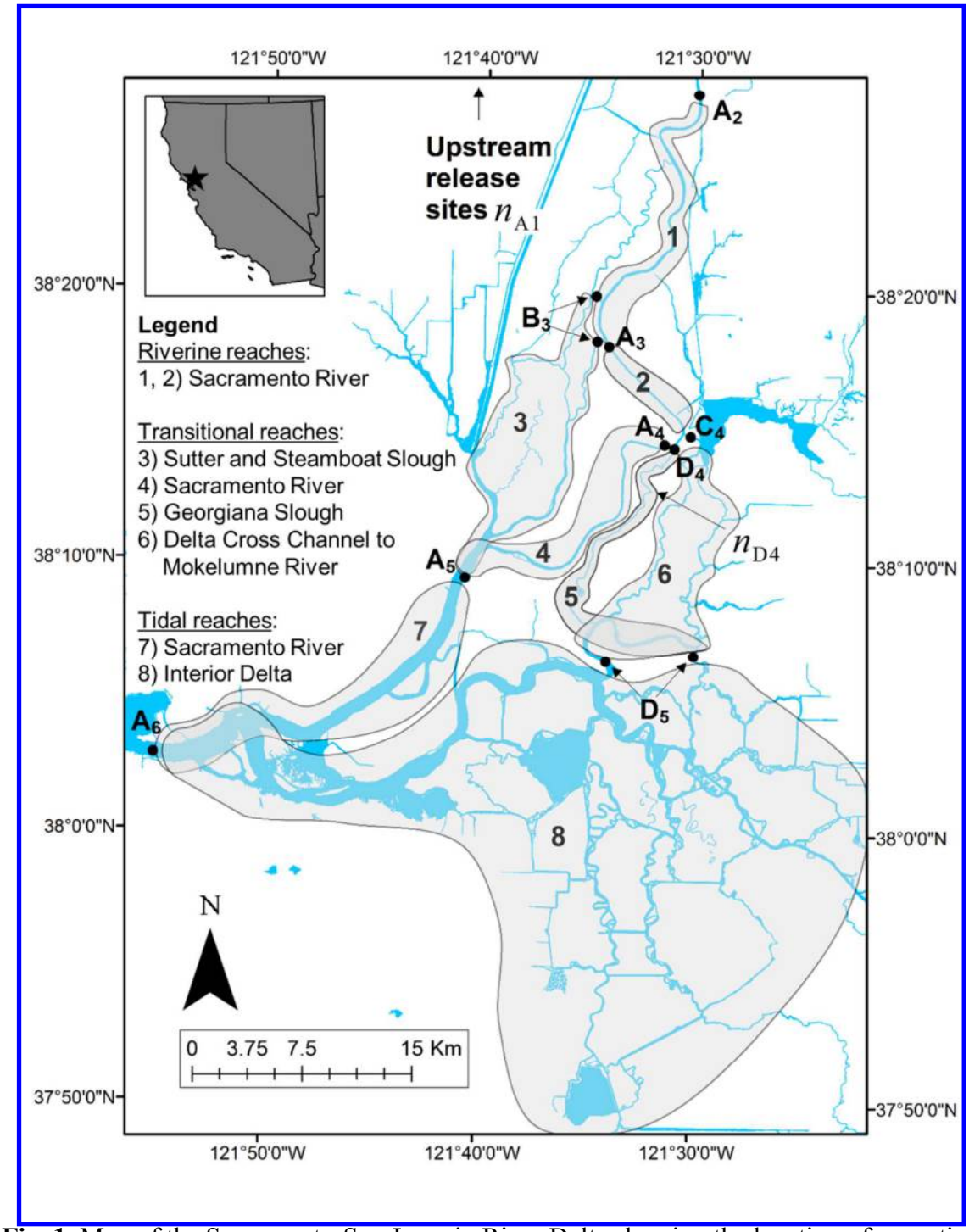

Fig. 1. Map of the Sacramento-San Joaquin River Delta showing the location of acoustic telemetry receiving stations (filled black circles) used to detect acoustic tagged juvenile salmon as they migrated through the Delta. Telemetry stations are labeled by migration route (A-D) and sampling occasion (1-7; see Fig. 2). These telemetry stations divide the Delta into eight discrete reaches (shown by numbered shaded regions), with an additional reach upstream of telemetry station A_2 (Reach 0) used as acclimation reach to allow fish to recover from post-release handling. The location of water pumping stations in the southern interior Delta is indicated by the pink diamonds.

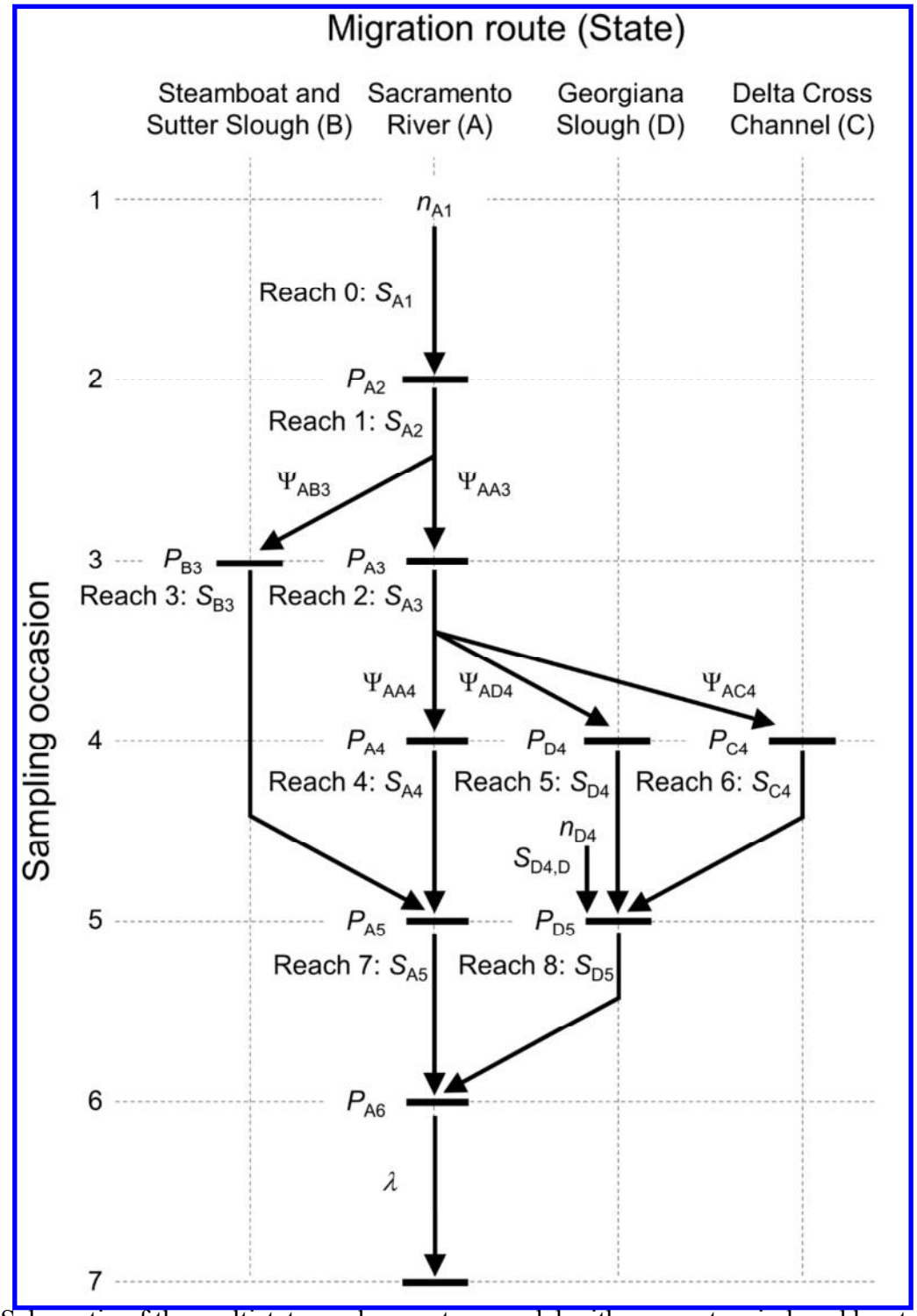

Fig. 2. Schematic of the multistate mark-recapture model with parameters indexed by state (migration route) and sampling occasion. Parameters include reach-specific survival probabilities (S), site-specific detection probabilities (P), routing probabilities (Ψ), and λ, the joint probability of surviving and being detected at telemetry stations downstream of site A_6. Release locations are indicated by the nth release in route r at occasion j: n_{A1} (at Sacramento or upstream – see Table 1) and n_{D4} in Georgiana Slough.

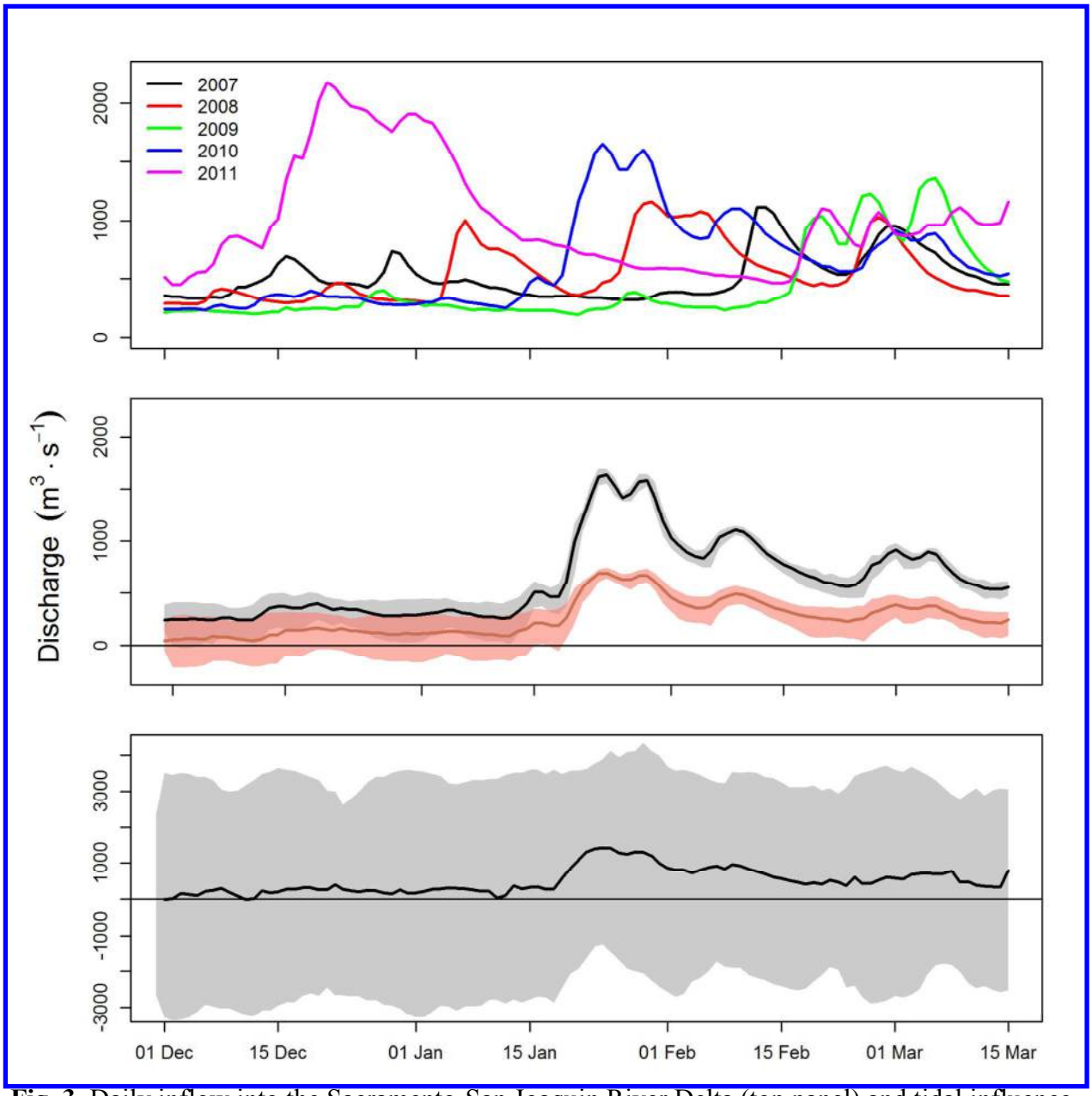

Fig. 3. Daily inflow into the Sacramento-San Joaquin River Delta (top panel) and tidal influence on discharge at three locations in the Sacramento River during 2010 (middle and bottom panels). The top panel shows mean daily discharge of the Sacramento River at Freeport (A_2 in Fig. 1). In the two lower panels, lines show mean daily discharge and the shaded regions encompass the daily minimum and maximum discharge with values less than zero indicating reverse flows caused by tidal forcing. The middle panel shows the Sacramento River at Freeport (black line, gray shading) and the Sacramento River just downstream of Georgiana Slough (pink link and shading; A_4 in Fig. 1). The bottom panel shows the Sacramento River at Rio Vista (A_5 in Fig. 1).

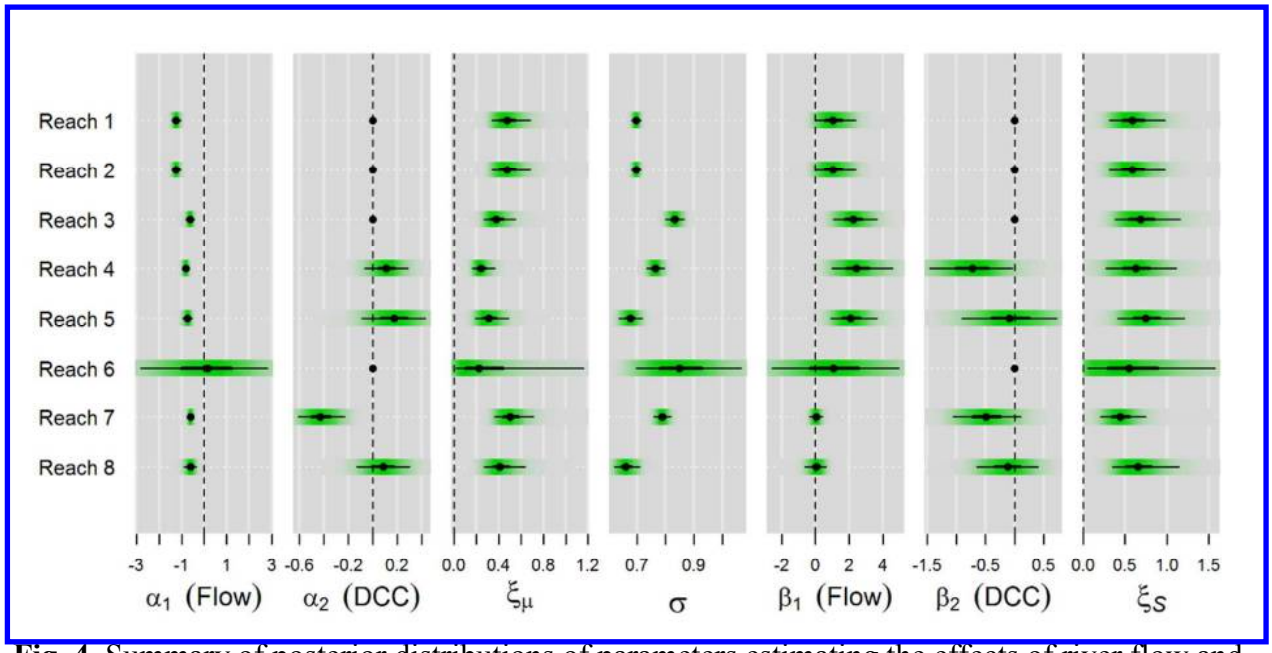

Fig. 4. Summary of posterior distributions of parameters estimating the effects of river flow and Delta Cross Channel (DCC) gate position on travel time and survival. Points show the median of the posterior distribution, heavy lines show the 25th to 75th percentile, and thin lines show the 5th to 95th percentile. Green bars are density strips with darker regions illustrating higher posterior density. Parameter definitions as follows: α_1 = slope for effect of discharge on mean of log-travel time, α_2 = slope for effect of an open DCC gate on mean of log-travel time, ξ_μ = standard deviation of release group random effect on μ, σ = variance parameter of the lognormal travel time distribution, β_1 = slope for effect of discharge on survival, β_2 = slope for effect of an open DCC gate on survival, ξ_S = standard deviation of release group random effect on survival.

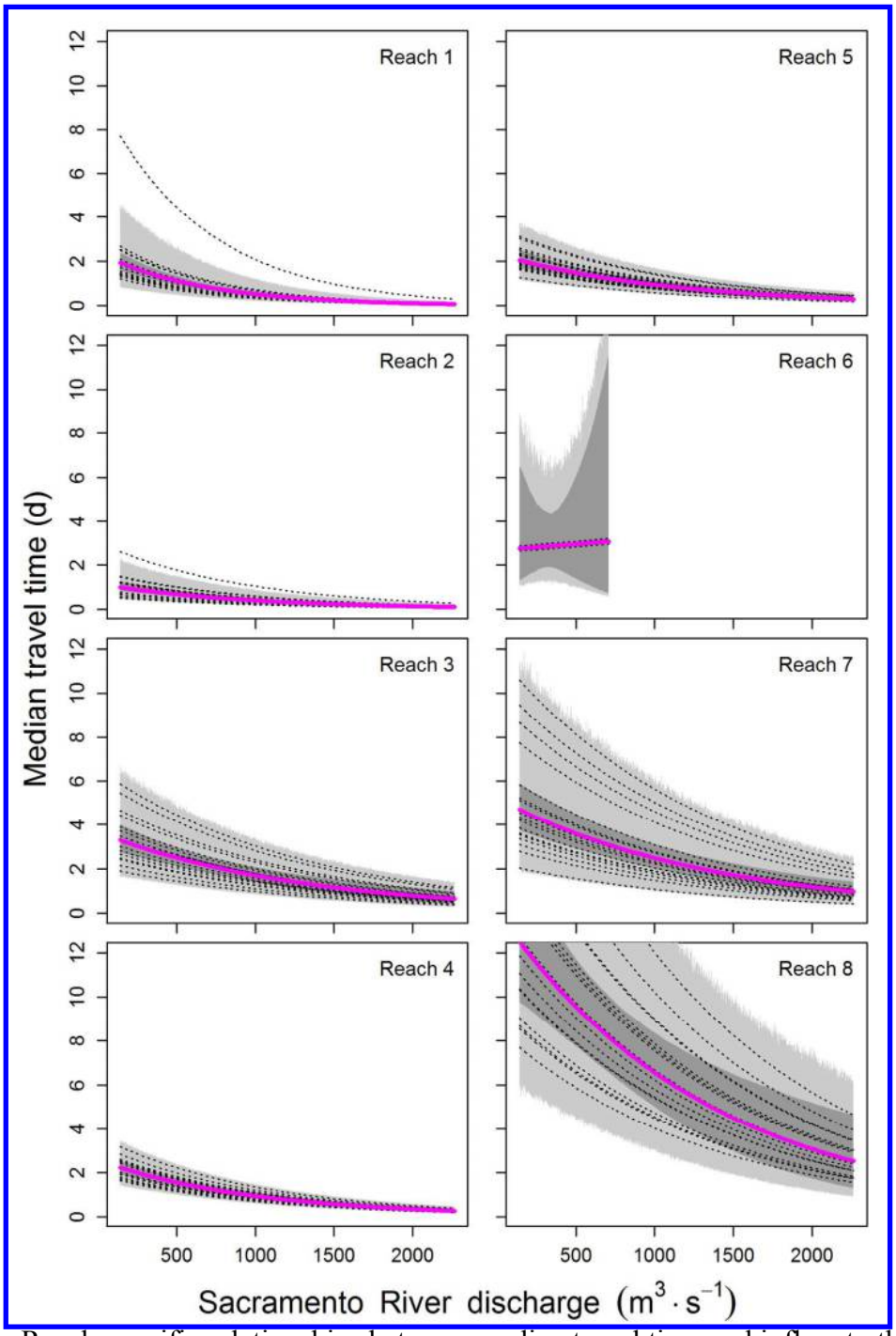

Fig. 5. Reach-specific relationships between median travel time and inflow to the Delta as measured at the Sacramento River at Freeport (A_2 in Fig. 1; shown for closed Delta Cross Channel gates and plotted at the mean fork length). The heavy magenta line shows the mean relationship and the dotted lines show the random effects estimates for each release group based on medians of the joint posterior distribution. The dark gray region shows 95% credible intervals about the mean relationship. The light gray region shows the 95% confidence interval among release groups.

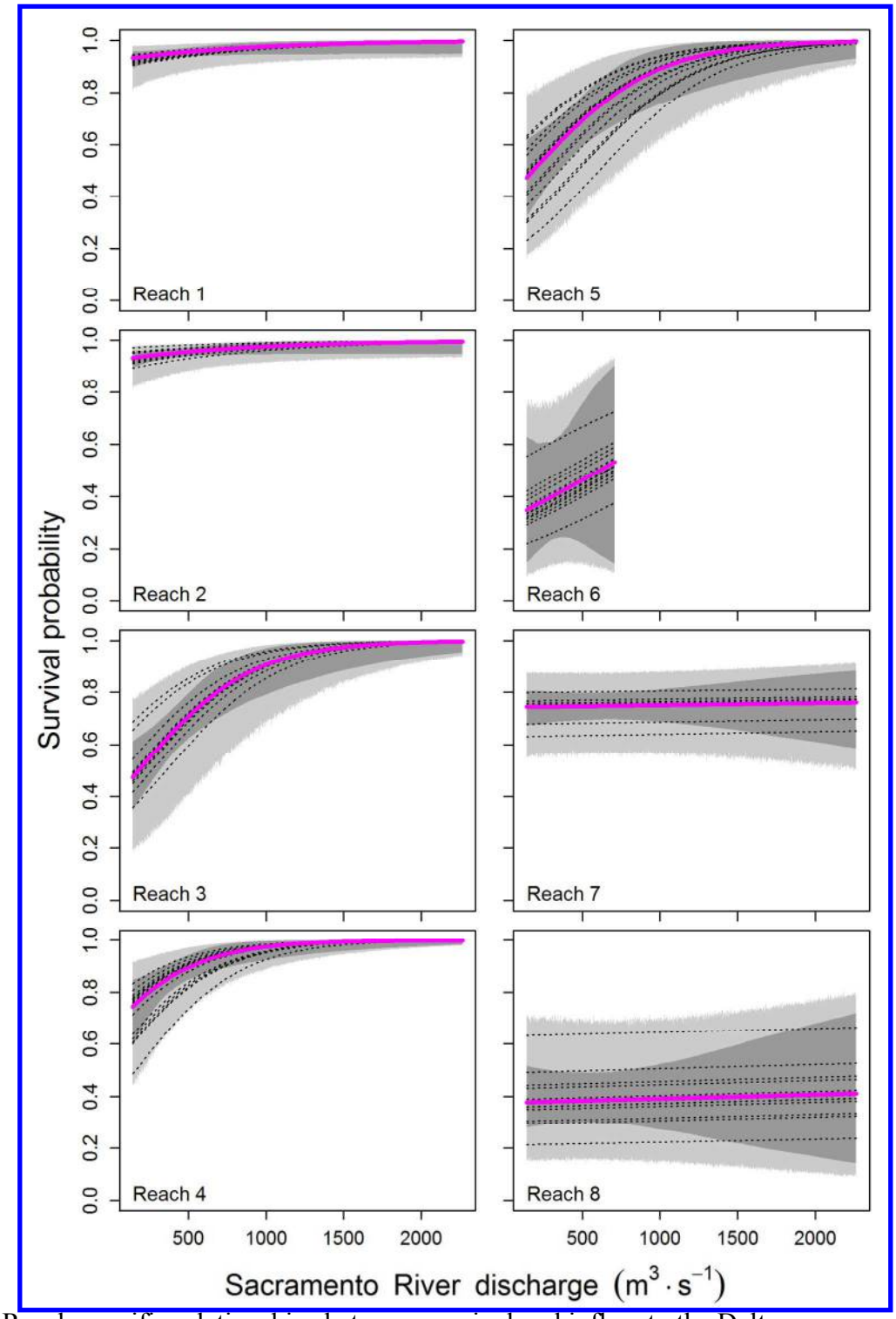

Fig. 6. Reach-specific relationships between survival and inflow to the Delta as measured at the Sacramento River at Freeport (A_2 in Fig. 1; shown for closed Delta Cross Channel gates and plotted at the mean fork length). The heavy magenta line shows the mean relationship and dotted lines show the random effects estimates for each release group based on medians of the joint posterior distribution. The dark gray region shows 95% credible intervals about the mean relationship. The light gray region shows the 95% confidence interval among release groups.

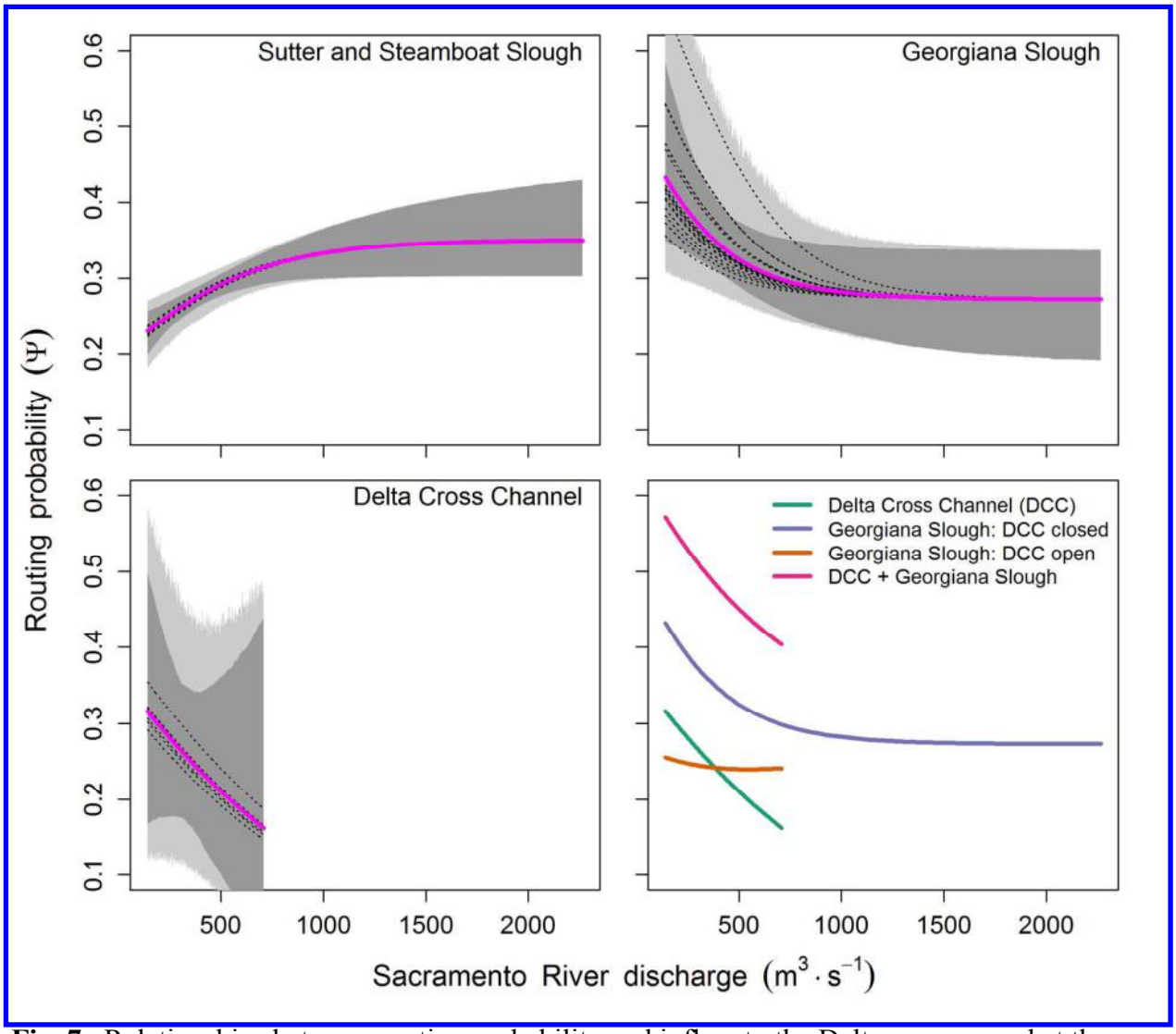

Fig. 7. Relationships between routing probability and inflow to the Delta as measured at the Sacramento River at Freeport (A_2 in Fig. 1). The lower right panel shows the effect of Delta Cross Channel (DCC) gate position on routing probabilities at the junction of the Sacramento River, Delta Cross Channel, and Georgiana Slough (A_4, C_4, and D_4 in Fig. 1), plotted at the posterior median of the parameters. Other panels show mean routing relationships (heavy magenta line), random effects estimates for each release group (dotted lines), 95% credible interval about the mean relationship (dark gray region), and 95% confidence interval among release groups (light gray region).

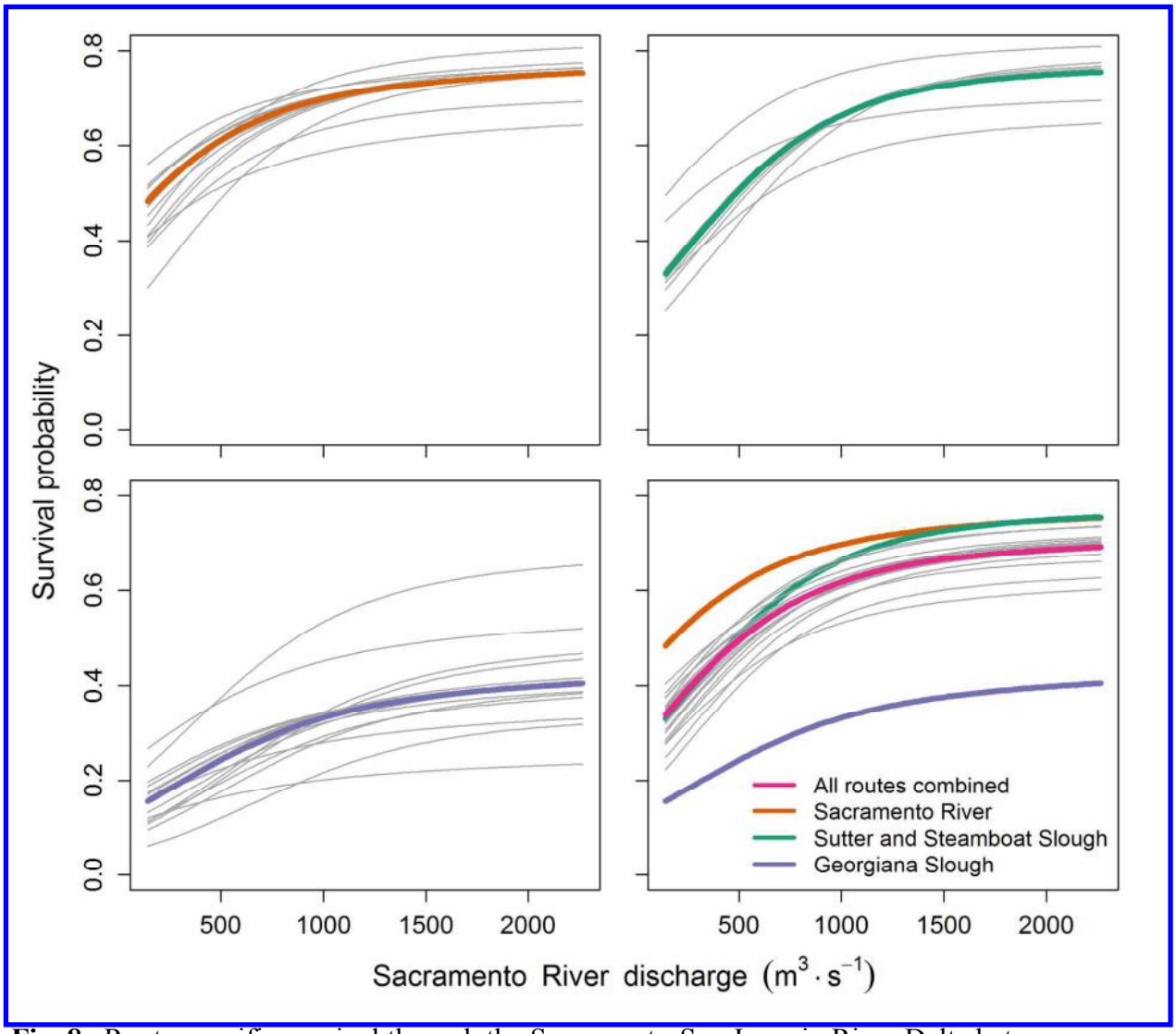

Fig. 8. Route-specific survival through the Sacramento-San Joaquin River Delta between Freeport (A_2 in Fig. 1) and Chipps Island (A_6 in Fig. 1). Route-specific survival based on posterior median parameter values was calculated as the product of reach-specific survival for reaches that trace each unique migration route through the Delta (shown for closed Delta Cross Channel gates). The first three panels show the mean relationship for each route with thin gray lines showing the random effects estimates for each release group. The last panel shows overall survival through Delta for all routes (with random effects estimates as thin gray lines) along with route-specific survival relationships. Overall survival was calculated as the average of route-specific survival weighted by routing probabilities (see Eq. 1).

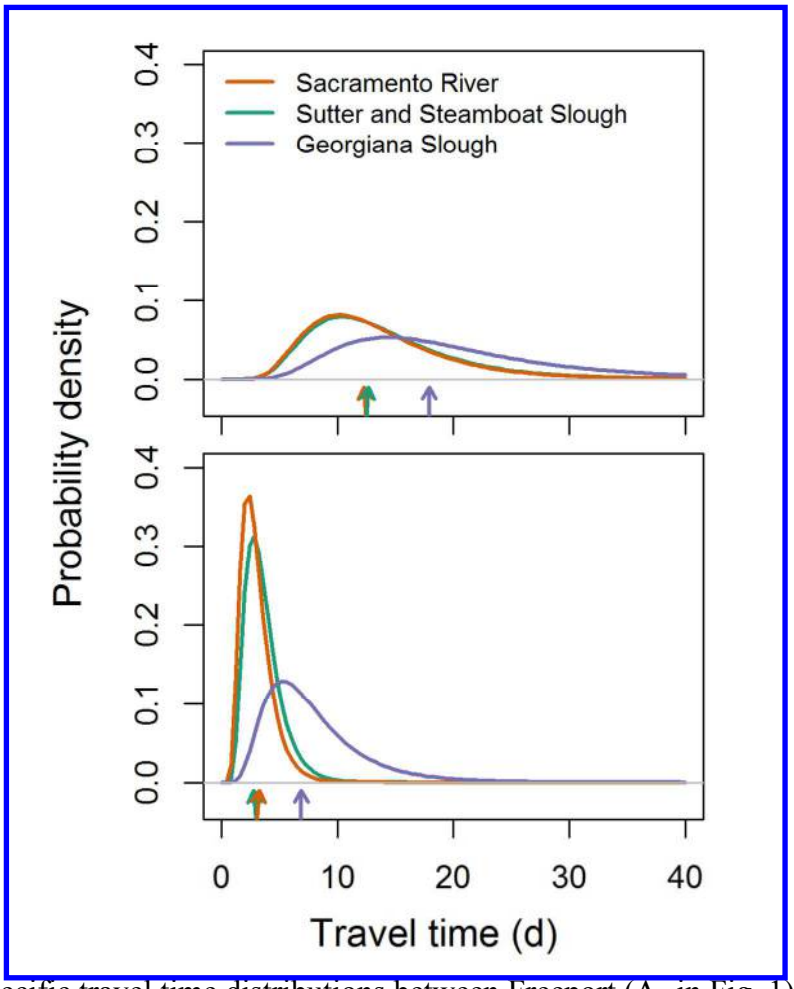

Fig. 9. Route-specific travel time distributions between Freeport (A_2 in Fig. 1) and Chipps Island (A_6 in Fig. 1) at the 5th (top panel) and 95th (bottom panel) percentiles of discharge based on the historical flow record (235 $m^3 \cdot s^{-1}$ and 1357 $m^3 \cdot s^{-1}$, respectively). Arrows show the median travel times for each route. Travel time distributions were based on posterior medians of parameters for reach-specific travel time distributions assuming closed Delta Cross Channel gates.